N69-35718
NASA CR-105395

R.P.I. Progress Report MP-4

A Progress Report for
July 1, 1968 to June 30, 1969

ANALYSIS AND DESIGN OF A CAPSULE LANDING SYSTEM AND SURFACE VEHICLE CONTROL SYSTEM FOR MARS EXPLORATION

National Aeronautics and Space Administration

Grant NGL-33-018-091

Submitted by the Special Projects Committee

D.K. Frederick
P.K. Lashmet
G.N. Sandor
C.N. Shen
E.J. Smith
S.W. Yerazunis

July 15, 1969

School of Engineering

Rensselaer Polytechnic Institute

ABSTRACT

Investigation of problems related to the landing and controlling of a mobile planetary vehicle according to a systematic plan of exploration of Mars has been undertaken. Problem areas receiving consideration include: updating of atmosphere parameters during entry, adaptive trajectory control, unpowered aerodynamic landing, terrain modeling and obstacle sensing, vehicle dynamics and attitude control, and chromatographic systems design concepts. The specific tasks which have been undertaken are defined and the progress which has been made during the interval July 1, 1968 to June 30, 1969 is summarized. Projections for work to be undertaken during the next six months period are included.

TABLE OF CONTENTS

Analysis and Design of a Capsule Landing System and Surface Vehicle Control System for Mars Exploration

I. Introduction

The planned exploration of the planet Mars in the 1970's involves the landing of an excursion module on the martian surface. Following a successful landing, the exploration of the martian surface would be promoted considerably if the excursion model is mobile and if its motion can be controlled according to a specific plan of exploration. Contributing to the formidable problems to be faced by such a mission are the existence of an atmosphere whose parameters are at this time rather uncertain within broad limits and the information transmission delay time between Martian and Earth control units. With the support of NASA Grant NGL-33-018-091, a number of important problems originating with the factors noted above have been investigated by a faculty-student team at Rensselaer.

The problems under study fall into two broad categories: (a) capsule landing and (b) control of a mobile exploration unit, from which a considerable number of specific tasks have been defined. This progress report describes the tasks which have been undertaken and documents the progress which has been achieved in the interval July 1, 1968 to June 30, 1969 and projects activity for the next period ending December 31, 1969.

II. Definition of Tasks

The uncertainty in martian atmosphere parameters and the delay time (order of ten minutes) in round trip communication between Mars and Earth underlie unique problems relevant to martian and/or other planetary explorations. All phases of the mission from landing the capsule in the neighborhood of a desired position to the systematic traversing of the surface and the attendant detection, measurement, and analytical operations must be consummated with a minimum of control and instruction by earth based units. The delay time requires that on board systems capable of making rational decisions be developed and that suitable precautions be taken against potential catastrophic failures such as vehicle flip-over. Five major task areas, which are in turn divided into appropriate sub-tasks, have been defined and are listed below.

A. Trajectory Control

A.1. Martian Atmosphere Updating - Uncertainty in

martian atmosphere parameters preclude a priori trajectory and landing specifications. The objective of this task is to develop methods for updating martian atmosphere parameters on the basis of measurements obtained during entry. The updated parameters will be used by an adaptive trajectory control system, Task A.2., and during unpowered aerodynamic landing, Task B.

A.2. Adaptive Trajectory Control - If updated martian atmosphere parameters can be obtained during entry, an adaptive trajectory control system can be used to achieve the desired velocity, range and altitude parameters prior to the final landing phase. This task is concerned with methods by which to achieve the desired terminal conditions given the availability of updated atmospheric parameters.

B. Unpowered Aerodynamic Landing. The existence of an atmosphere on Mars, slight as it is, offers an opportunity for unpowered landing of the capsule through the use of aerodynamic forces. The objective of this task is to investigate the feasibility of devices utilizing aerodynamic forces to effect an acceptable landing approach and touchdown.

C. Surface Navigation and Path Control. Once the capsule is landed and the roving vehicle is in an operational state, it is necessary that the vehicle can be directed to proceed under remote control from the landing site to specified positions on the martian surface. This task is concerned with the problems of terrain modeling, path selection and navigation between the initial and terminal sites when major terrain features precluding direct paths are to be anticipated. On board decision making capability must be designed to minimize earth control responsibility except in the most adverse circumstances.

C.1. Terrain Sensing - The problem of gross navigation and path selection, requires major terrain feature information. The objective of this task is to define a system which will provide the required information describing the surrounding terrain to permit path selection decisions to be made.

C.2. Short Range Obstacle Sensing and Avoidance - It can be expected that many minor obstacles will be encountered by a roving vehicle. The objective of this task is to investigate and define methods of short range obstacle detection to provide the information necessary for steering maneuvering control components to avoid such obstacles and to allow the gross navigation plan to be implemented.

D. Vehicle Dynamics and Attitude Detection System

D.1. Vehicle Dynamics - As the vehicle negotiates the martian surface according to periodic instructions from Earth, it will encounter an uncertain terrain. Depending on the apparatus, instruments and devices with which the vehicle is equipped to meet mission objectives, particular requirements as to vehicle reaction, i.e., forces, orientation, etc., to the terrain may have to be satisfied. In addition, the response of the vehicle to potential terrain features of appropriate scale and repetitious nature must not be unacceptable. The objective of this task is to establish vehicle parameters, i.e., dimensions, arrangements, suspension details, satisfying mission requirements.

D.2. Attitude Detection Systems - Effective attitude detection systems will be required not only while the vehicle is stationary to permit planned experimentation to be undertaken and to make essential terrain measurements but also when the vehicle is in motion to provide information for the effective interpretation of obstacle detector signals and to provide alarms if the slope of the local terrain approaches critical values.

E. Chemical Analysis of Specimens.

A major objective of martian surface exploration will be to obtain chemical, biochemical or biological information. Most experiments proposed for the mission require a general duty, chromatographic separator prior to chemical analysis by some device. The objective of this task is to generate fundamental data and concepts required to optimize such a chromatographic separator according to the anticipated mission.

The tasks defined above have been pursued by a team of six faculty members and twenty-two students. Of this group of students, ten have received some financial support from the project while the remainder are participating without remuneration in order to fulfill their academic requirement of engineering project. Details of the student team including their degree objectives and achievements, and support relationship are given in Section V. Sections III and IV which follow summarize the progress which has been made during the prior period and project activities for the coming year, July 1, 1969 to June 30, 1970.

III. Summary of Results

Task A. Trajectory Control

The control of trajectory prior to the final landing phase involves two major problem areas both of which originate with the present uncertainties of the parameters of the martian atmosphere. The first of these areas is concerned with the development of methods by which to update the atmosphere parameters during entry and an assessment of the implications of measurement errors. The second of these areas is related to trajectory control in terms of terminal velocity using thrust or drag devices to permit for a proper transition into the final landing phase.

Task A.1. Updating of Martian Atmosphere Parameters -

R.J. Carron, R.E. Janosko, and J.R. Morgan
Faculty Advisor: Prof. C.N. Shen

This task is concerned with the development and evaluation of methods by which to determine martian atmosphere parameters during entry. These parameters would be used by an adaptive control system, Task A.2., to achieve the desired terminal conditions of velocity, altitude and range angle for the entry vehicle prior to the final landing phase, Task B.

The initial effort was focused on a method updating the parameters of a modified adiabatic density model applying to that region of the atmosphere below the tropopause, Ref. 1. Since the non-conventional techniques which have been suggested for vehicle trajectory control (Ref. 2,3) require knowledge of the atmospheric parameters at altitudes above the tropopause, several additional efforts have been undertaken to

extend the scheme to higher altitudes. In addition, the method of updating parameters described in Ref. 1 has been applied to the trajectory control scheme outlined in Ref. 2. Details of these activities are summarized below.

1. Updating of Parameters for the Region below the Tropopause

The general approach to the problem can be summarized as follows. The entry vehicle is presumed to be instrumented so as to provide density-altitude data at appropriate intervals during the trajectory. These data are then used to modify the parameters of the adiabatic atmospheric model below the tropopause. The particular scheme which has been developed uses a transformed form of the adiabatic equation with the independent variable, altitude, in a modified form so as to track in the direction of travel. The problem of minimizing the effect of measurement error was investigated from a statistical viewpoint and the method of modified least squares was selected as the solution to this problem.

Computer results simulating the descent from the tropopause height of a design atmosphere to the surface indicate that the scheme does update the parameters properly. The parameters converge rapidly from their reference values to those of the actual atmosphere as seen in Figures 1 and 2.

It was found that the parameter weights used in the modified least squares solution greatly affect the performance of the system. The behavior of the system can be controlled by proper manipulation of these weights, Ref.(4,5). A detailed technical report on this method is provided in Ref. 1.

2. Extension to Regions Above the Tropopause

Although the scheme outlined above was shown to be effective in using measured data with error to modify atmosphere parameters from an initially assumed reference atmosphere to those for the actual atmosphere, it is limited in its application to only the region of the atmosphere below the tropopause. Accordingly, efforts were made to seek methods by which to use data to be obtained during entry above the tropopause to establish the atmosphere at an earlier time in the entry processes. Unfortunately, none of the schemes which were conceived and tested proved to be satisfactory.

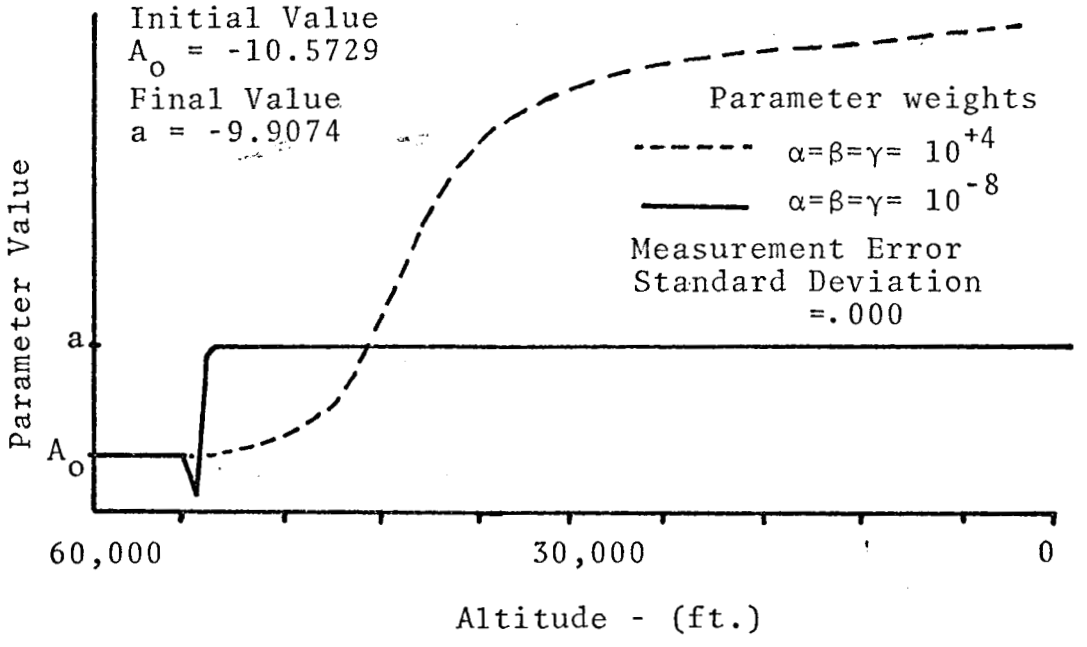

Figure 1

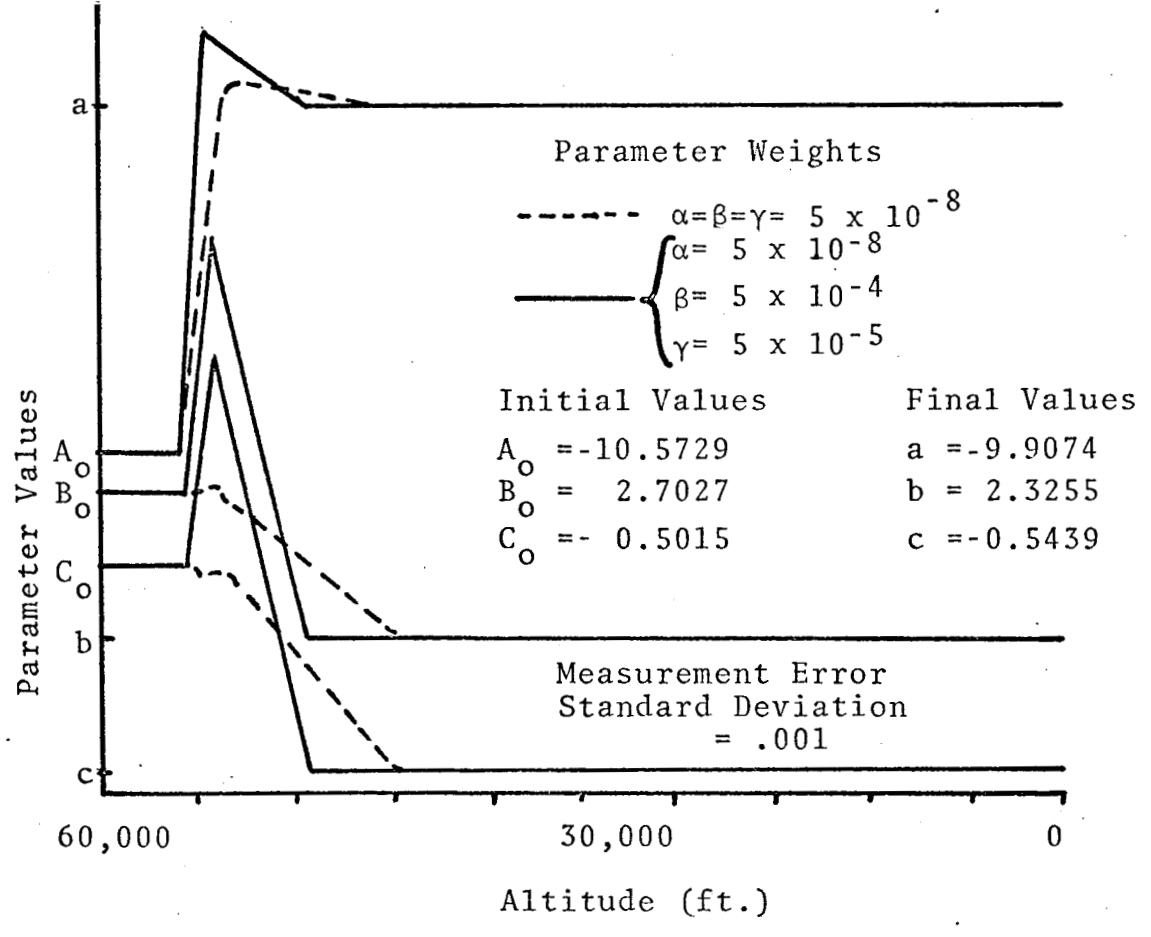

Figure 2

Nevertheless, the knowledge which was gained does provide some use insights of the problem.

Two of the main thrusts were based on off-line schemes. One of these sought to find functional relationships between the altitude and those "adiabatic"* parameters fitting the atmosphere in the exponential region, i.e. above the tropopause. It was hoped that such relationships would define the atmospheric models uniquely and that early (i.e. high altitude) measurements would provide a basis for predicting the actual atmosphere. These hopes did not materialize. The second approach attempted to match the coefficients of equal powers after the exponential and adiabatic models had been expanded in power series. Such a correlation would have permitted a prediction of the complete atmosphere using high altitude measurements. However, the coefficients which were derived were inconsistent and efforts to minimize errors resulted in excessively complex formulations of dubious potential.

At this point, the effort was turned to an on-line parameter updating study which was a direct extension of the original scheme, Ref. 1, differing only in two respects: a) all of the measured data obtained both above and below the tropopause were used and b) a weighting system favoring later points (i.e. lower altitude data) was included. In testing this method it was found that with suitable weighting, convergence to the correct parameters was obtained; however, the convergence was slow and no advantage over the original scheme, Ref. 1 was perceived.

3. Application of Parameter Updating Scheme to Adaptive Trajectory Control System

The parameter updating scheme, Ref. 1, was applied to the sensitivity guidance control technique, Task 2.A., described in Ref. 2, to determine the effectiveness of the overall method and to assess the significance of atmosphere property measurement error. The effects of measurement error are twofold. First, there is a delay in the updating scheme in converging to the true values.

* Since the density of the atmosphere above the tropopause is expected to be related to altitude by a two-parameter exponential model, its correlation by a three-parameter adiabatic model can only produce equivalent adiabatic parameters which lack the physical significance of those applying below the tropopause.

Second, there is the error in the final values once steady state conditions are reached due to the measurement errors. The first error causes the control scheme to converge to the terminal state slower than with immediate updating. The second causes errors in the predicted terminal states.

An effective control scheme is one which converges to the desired final values before the craft arrives at the terminal height and does not deviate significantly from desired terminal conditions because of measurement errors.

The adaptive control simulation program, Ref. 2, has been modified so as to use the original parameter updating scheme and encouraging results have been obtained. The results for a simulation in which a VM-1 reference atmosphere was assumed along with a VM-2 actual atmosphere are shown in Fig. 3 and 4. For a standard deviation in measurement of 0.004, the percent deviation in final states between the cases with and without measurement error is 0.2%, i.e. the error is halved by the adaptive control system.

It should be noted that the optimal weighting parameters employed in the updating scheme are a function of the particulars of the reference and actual atmosphere involved. The weights used in above simulation differ from those deduced for the VM-4: VM-8 situation studied in detail in Ref. 1. Since the principal effect of non-optimal weights is to reduce the rate of convergence to correct parameters, it remains to develop rational techniques for adjusting the weights.

In addition, it should be noted that this simulation assumed that the actual atmosphere could be described by the adiabatic model up to the altitude of 90,000 feet at which control action was initiated. This is believed to be a good approximation for the case involved.

It should be mentioned that a measurement error as large as 10% was also used in the simulation. The updating scheme behaved well and the terminal errors were of the same magnitude as those obtained with a 4% measurement error. This indicates that the relationship between measurement error and terminal state error is not a direct proportional relationship and that measurement error is not critical.

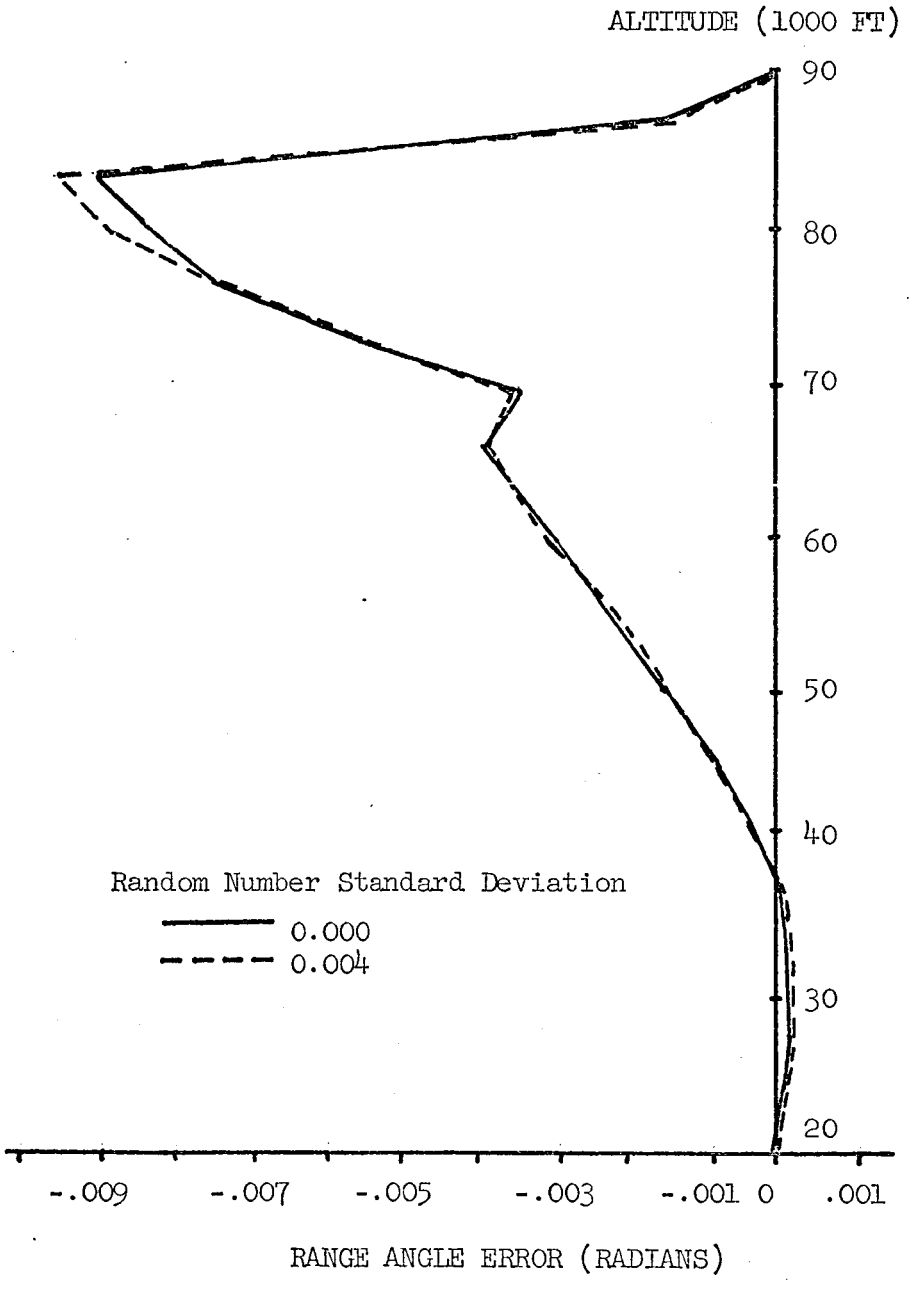

Fig. 3. Predicted Deviation in Velocity at 20,000 ft vs. Altitude

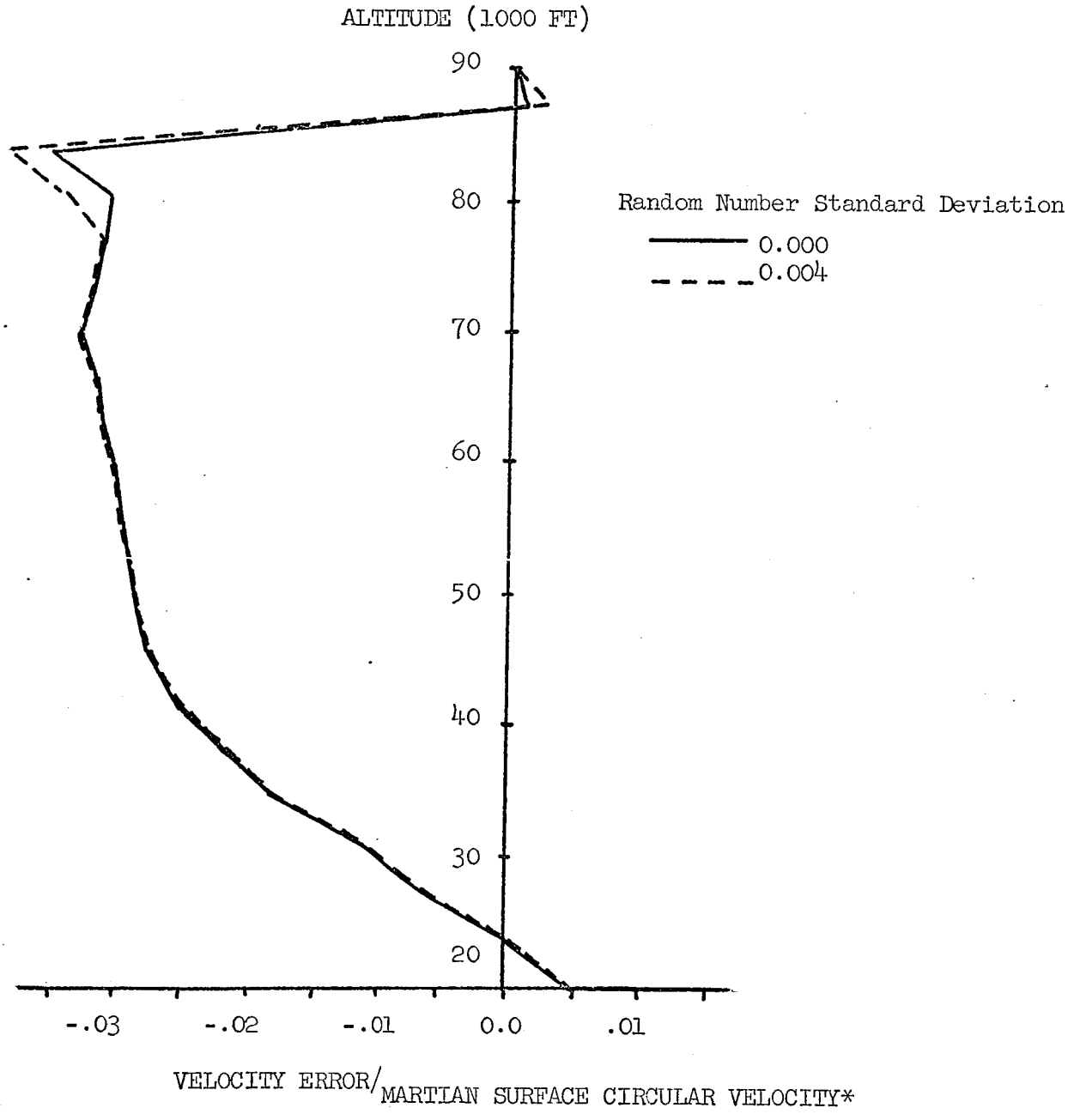

Fig. 4 Predicted Deviation in Velocity at 20,000 ft vs. Altitude

* Martian Surface Circular Velocity = 11,558 ft/sec

It is concluded that the combined control and updating scheme can, with some improvements, provide the required trajectory control.

Task A.2. Adaptive Trajectory Control

Principal efforts have been directed along two lines. The first of these has been concerned with the development of methods by which to compute the effects of both density parameter deviations and retro-propulsion control changes and has resulted in the formulation of a technique based on sensitivity analysis. The second line of effort has considered trajectory control in terms of discrete variation of the ballistic coefficient.

Task A.2.a. Sensitivity Guidance for Entry into an Uncertain Martian Atmosphere - P.J. Cefola
Faculty Advisor: Prof. C.N. Shen

The objective was to develop a guidance scheme which would result in a reference terminal condition, i.e. capsule velocity and range angle at a specified altitude, whatever the actual atmosphere encountered on Mars entry. It is assumed that an on-board system for updating atmosphere parameters is available.

Sensitivity Analysis is applied to the entry dynamics in order to compute the effects of both density parameter deviations and control changes. After the atmospheric parameters are tracked, the control is determined on-board by using the sensitivity coefficients previously compiled. Control updating is provided by introducing a new sensitivity equation which reduces the on-board computation since all the required terminal sensitivity coefficients are now produced by the solution of one equation. Numerical simulation assuming a VM-2 reference density and VM-1 actual density showed that the terminal velocity and range angle errors were reduced by at least 90% in comparison with those resulting from the uncontrolled VM-1 trajectory. The effects of delays in obtaining information describing the actual atmosphere and of inaccuracies in that information were also investigated.

Second order sensitivity functions are investigated with a view towards improving guidance system performance in the case of large deviations in the atmospheric parameters. Previous workers have derived higher order

sensitivity equations using a single n-th order differential equation to model the physical system. However, the state vector described by n first order equations gives a more general approach for dynamical systems. A new vector-matrix differential equation for the second order sensitivity coefficients of a general system is obtained. It is found that the second order sensitivity forcing function depends on the present altitude in a planetary entry problem in contrast to the first order sensitivity forcing function which is independent of the present altitude. This point is important in the calculation of the terminal values of the second order sensitivity coefficients. With the first order coefficients, it was possible to describe all the terminal values by using the adjoint sensitivity equation. For the second order coefficients, this procedure is only possible for a certain approximation to the second order sensitivity forcing function.

Ref. 2 describes in detail the development and application of the proposed guidance scheme.

Task A.2.b. Adaptive Trajectory Control with Discrete Change in Ballistic Coefficient and a Sequence of Discrete Changes in Flight Path Angle - L. Hedge
Faculty Advisor: Prof. C.N. Shen

The entry guidance system for a Martian vehicle must meet certain terminal constraints at a terminal altitude if the soft landing of the capsule on the surface is to be successful. However, due to the existing uncertainty in the actual characteristics of the Martian atmosphere, the guidance system must be able to compensate for deviations from the assumed reference atmosphere. Trajectories obtained from aerodynamic breaking are particularly sensitive to actual atmosphere. Deviations in the atmospheric parameters which describe the atmosphere cause important changes in the terminal conditions; and according to present estimates, the parameter deviations may be quite large.

Since the density of the Mars atmosphere is much lower than that found on Earth, and the aerodynamic drag on the entry capsule is proportionately lower, two techniques have been suggested. They are: (i) altering the ballistic coefficient of the vehicle, and (ii) lengthening (or shortening)the flight path in the atmosphere. Therefore, for controls in a guidance scheme which compensates for the atmospheric uncertainty of Mars, this

investigation has been concerned with using: (i), a discrete change in the ballistic coefficient (m/C_DA) by altering the effect surface area of drag (A), and (ii), a sequence of small discrete changes in the flight path angle by applying an impulsive force perpendicular to the direction of the velocity.

Assuming a knowledge of the reference atmospheric parameters and a method of tracking the actual parameters, the approach to the problem has been to find an altitude for changing the drag surface which minimizes the deviation of the actual terminal conditions from the reference terminal conditions. The sequence of impulsive changes in the flight path angle can then be employed as a trim to reduce the remaining errors in the actual final conditions.

A reference value for the ballistic coefficient has been established by NASA (.30 slugs/ft^2). To determine the effect of a change in the drag surface on the final values of the state variables, the area ratio was varied as a function of altitude. Simulating this procedure over the range of possible atmospheres determined the values of the area ratio necessary to compensate for deviations from a reference set of atmospheric parameters. It also determined the altitude at which the ballistic coefficient is changed as a function of actual atmosphere.

However, the accuracy of such a procedure is dependent on the accuracy of the actual atmospheric parameters from an updating scheme when the change in area is made. If improved values of the parameters are obtained after the ballistic coefficient is changed, a sequence of discrete changes in the flight path angle may be used to minimize the resulting state variable errors.

It has been found that such a proposed guidance scheme is able to compensate for a certain range of atmospheric parameter deviation. From a good estimate of the atmospheric composition, a reference trajectory can be chosen which has the required terminal conditions. Then based upon small deviations in the reference parameters, the ballistic coefficients can be altered so that the terminal conditions are satisfied. Then if inaccurate estimates of the actual atmospheric parameters exist at the altitude of change in the drag surface, the terminal errors which result may be corrected by small step changes in the flight path angle of the vehicle.

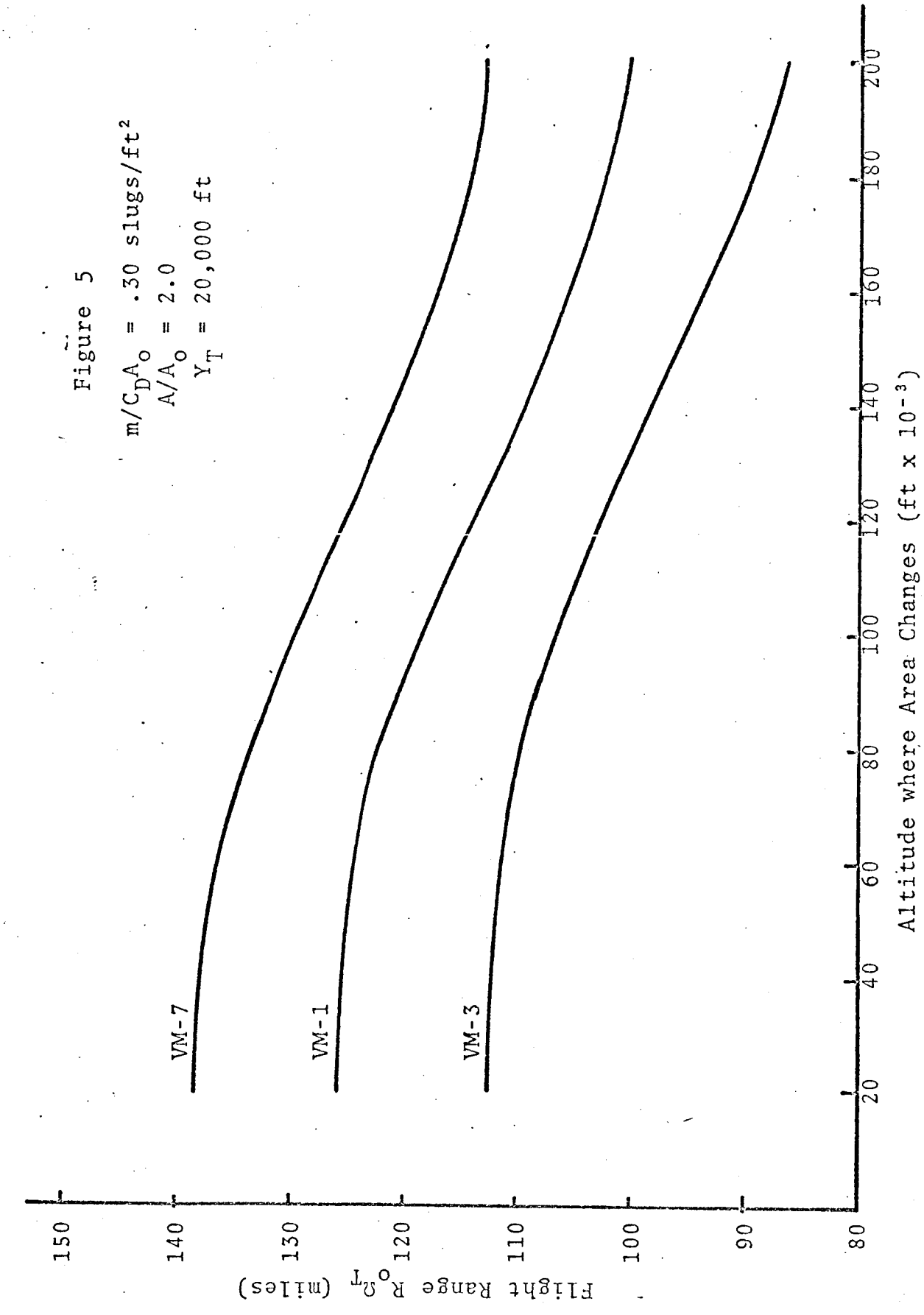

Figure 5

$m/C_D A_o$ = .30 slugs/ft^2
A/A_o = 2.0
Y_T = 20,000 ft

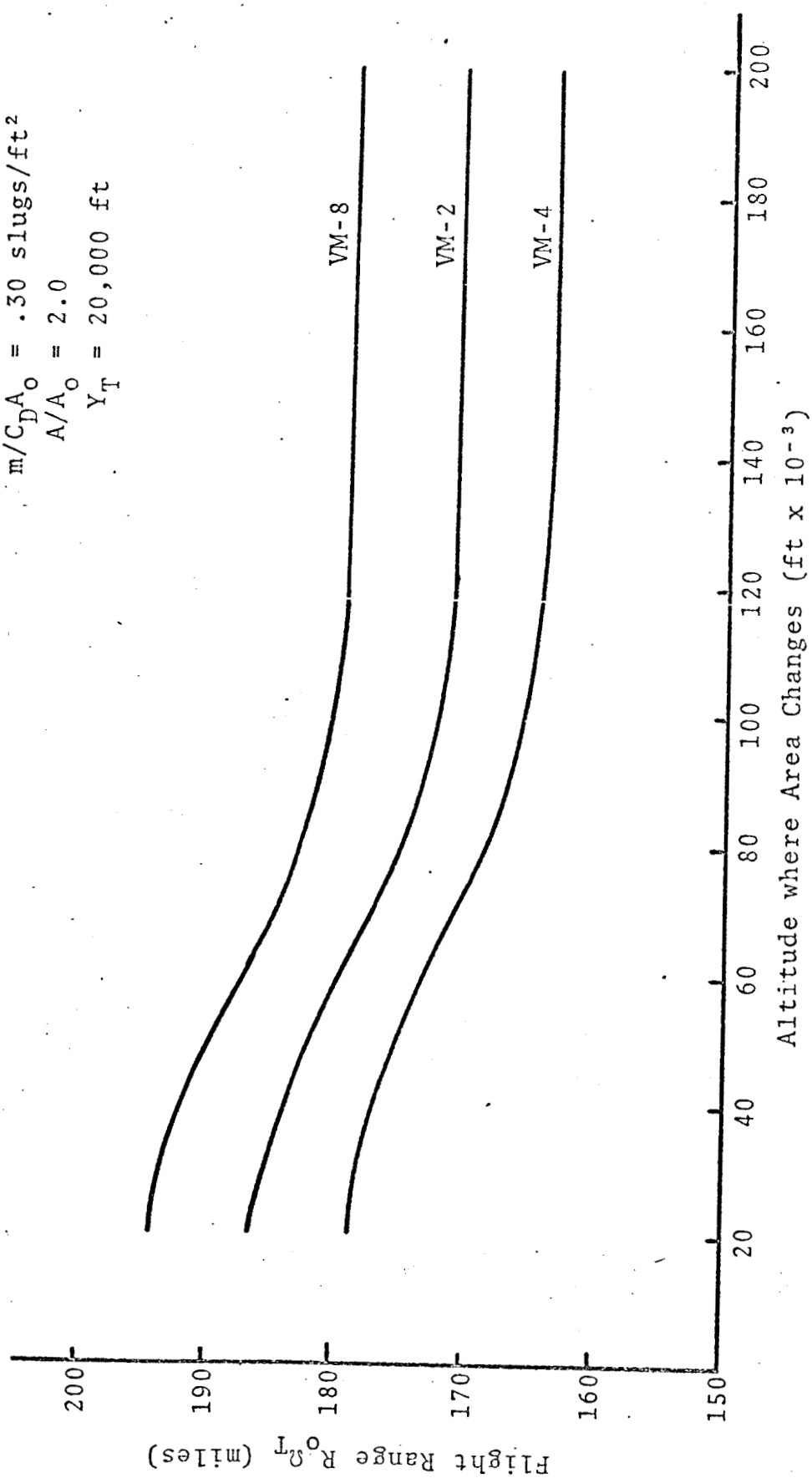

Figure 6

m/C_DA_o = .30 slugs/ft²
A/A_o = 2.0
Y_T = 20,000 ft

TYPE OF CONTROL		ALTITUDE OF UPDATE			
		76,000 ft.	62,000 ft.	48,000 ft.	34,000 ft.
UNBOUNDED	PREDICTED $\Delta\Omega(x_T)$ (rad)	-.00129	+.000730	+.000514	+.000228
	$\Delta\Theta_c(s)$ (rad)	-.0331	+.0542	+.1293	+.1510
	$V_c(s)$ (ft/sec)	- 282	+ 245	+ 195	+ 110
BOUNDED $\lvert\Delta\Theta_c(s)\rvert$ <.01	PREDICTED $\Delta\Omega(x_T)$ (rad)	-.00129	-.000341	+.000272	+.000408
	$\Delta\Theta_c(s)$ (rad)	-.01	-.01	+.01	+.01
	$V_c(s)$ (ft/sec)	- 85	- 40	+ 15	+ 8
BOUNDED $\lvert\Delta\Theta_c(s)\rvert$ <.015	PREDICTED $\Delta\Omega(x_T)$ (rad)	-.00129	-.000126	+.000468	+.000588
	$\Delta\Theta_c(s)$ (rad)	-.015	-.00936	+.015	+.015
	$V_c(s)$ (ft/sec)	- 128	- 38	+ 23	+ 11

TABLE 1

	FLIGHT RANGE ERROR
NO CONTROL	-22,500 yds
WITH DRAG CONTROL AT 89,400 ft.	- 6,000 yds
WITH UN-BOUNDED TRIM	+ 90 yds
WITH BOUNDED TRIM $\lvert\Delta\Theta_c\rvert$<.01	+ 1.300 yds
WITH BOUNDED TRIM $\lvert\Delta\Theta_c\rvert$<.015	+ 2,200 yds

TABLE 2

Legend

$\Delta\Omega(x_T)$ Terminal range angle deviation
$\Delta\Theta_c(s)$ Flight path angle correction
$V_c(s)$ Velocity correction (normal to flight path)

If the final velocity constraint is considered as an inequality, it is only necessary to keep the ballistic coefficient less than .30 slugs/ft^2 to insure that terminal velocity at twenty thousand feet above the surface is less than one thousand feet per second. Therefore, the changing of the drag surface area need only be employed to make the capsule reach a reference range point.

If the composition of the actual atmosphere is similar to that of the assumed reference atmosphere, there exists an altitude at which changing the drag surface by a factor of two will result in zero range error (see Fig. 5 and 6). However, if the actual atmospheric composition differs greatly from the reference atmosphere, the reference range can only be reached by a change in the ballistic coefficient which is much greater than a factor of two. The flight range for unpowered aerodynamic entry is extremely sensitive to the composition of the atmosphere. Therefore, a drag control scheme alone is sufficient only if a good estimate of the atmospheric composition is known before the mission.

It has also been found that a sequence of discrete changes in the flight path angle is very effective in reducing small errors due to changing the ballistic coefficient at the wrong altitude. Both bounded and unbounded control have been considered and a comparison of the two methods is important, Tables 1 and 2. The change in the ballistic coefficient was used to reduce an uncontrolled error of twenty two thousand yards to only six thousand yards. This is for a VM-8 reference atmosphere, VM-4 actual atmosphere, and changing the ballistic coefficient by a factor of two.

The range error using four corrections of unbounded magnitude is reduced from six thousand yards to only ninety yards. However the velocity changes necessary at each altitude are quite large for a vehicle which will weigh approximately five thousand pounds. They range from two hundred and eighty two feet per second for the first correction to one hundred and ten feet per second for the fourth correction, Table 1.

A bounded step change seems to be a much better solution from both the numerical results and physical limitations. The range error for bounded control is larger than that for unbounded control. However, the error for a bound of one hundredth of a radian is still

less than one mile. More important is the fact that the magnitude of the velocity changes are very small, especially when compared to the velocity changes necessary for unbounded control. For a bound of .01 radians, the velocities range from eighty five feet per second to eight feet per second.

Details of this study are provided in Reference 3.

Task B. Unpowered Aerodynamic Landing

Accomplishing a soft landing on the planet Mars can be a particularly difficult mission. The atmosphere of the planet is so tenuous (surface density on the order of 100-th the density of that of Earth's) that the techniques employed for Earth re-entry seem by themselves inadequate. These proposed methods of soft landing usually employ a large, blunt body for entry, parachute, balloon, or deployable wing for descent, and retrothrust rockets for soft touchdown.

The combined weight of such a system would tend to preclude the development of small landing capsules due to a very unfavorable payload fraction. On Mars the difficulties are aggravated by the existence of extremely high surface winds (200 ft/sec. with higher gusts). A soft landing capsule must be able to counteract these winds so as to land at zero ground speed. While flight into a headwind at zero ground speed would impose extra fuel requirements on a retrothrust-supported landing vehicle, it will actually improve the performance of a device which employs aerodynamic lift for support, such as the autogyro.

The unpowered rotary wing, which seems to be the best aerodynamic means of providing the deceleration during descent and of countering the surface wind, offers the advantage that kinetic energy can be stored in the rotating hub and wing assembly. This makes it possible to hover briefly before touchdown without expending fuel, and make contact with the ground very rapidly.

This task involves a number of phases which are considered separately below and includes problems in: descent simulation, analysis of transient blade motion, hub design, blade pitch control system, design and fabrication of inflatable blade section, and aerothermoelastic blade analysis.

Task B.1. Descent Simulation Including Transient Blade Analysis - T.N. Kershaw
Faculty Advisor: Prof. G.N. Sandor

Evaluation of the feasibility of the unpowered rotary wing concept as an alternative to more conventional schemes for controlled deceleration and soft landing requires that methods for obtaining reliable descent simulations be developed. The progress which has been achieved towards this goal of reliable descent simulations is summarized below.

Blade element theory has been employed to develop the mathematical description of the performance of a rigid rotor during descent. These relationships are more useful than those previously reported in the literature since they result in closed form solutions for performance over a wide range of flight conditions, expected to be encountered in entry.

The efforts during the past period associated with the task of determining the operating characteristics of the rotor can be summarized as follows:

1. A state-of-the-art survey of rotor performance analyses has been made and the results are tabulated in Table 3. This tabulation indicates that while the present efforts are not the most general of those available, they do provide closed form solutions of steady state autorotation and are therefore more informative.

2. The equations for the coning angle, β , have been developed and incorporated into a computer program. Results from early calculations indicate that a coning angle on the order of 10 to 25 degrees can be expected during the descent.

3. The sensitivity of the flight performance to the tip-loss factor, B, has been investigated and found to be minor for the large range of inflow ratios, Table 4. Thus, the error due to using an inexact tip-loss factor is of minor concern.

4. The descent simulation equations and their associated assumptions for a rigid rotor with flapping hinge have been reviewed. Separate computer programs have been developed to check the various simulation calculations. These programs employ

TABLE 3. COMPARISON OF CALCULATED METHODS

	(1)	(2)	(3)	(4)	(5)*
Linearly varying pitch	I	I	I	I	I
Tip loss factor	I	I	I	I	I
Flapping motion	N	I:2nd order	I:2nd order	I	I: 2nd ord.
Drag contribution to lift	N	I:N forward vel region	I:(?)	I	I
Local induced vel.	N	N	A: mean	I	N
Transient blade motion	N	N	N	I	N
Coning angle, β	A:small	A:small	I	I	I
Inflow angle, ϕ	A:small	I:A small	I	I	I
Coefficient of lift, C_L	A:= $a\alpha_r$	A: $a\alpha_r = K_1$	I	I	$I_{F.S.}$
Coefficient of drag, C_D	(A:$\bar{c}_d$)	(A: $\delta_0 + \delta_1\alpha_r + \delta_2\alpha_r^2$)	I	I	$I_{F.S.}$
Angle of attack, α_r	A:small	A:small	A:moderate in use	I	I
Chord width		A:const	A:const	I	I,A:const
Lead-lag hinge	N	N	N	I	N

* (1) Wheatley 1934
(2) Gessow and Crim 1951
(3) Tanner 1964
(4) Present analysis, axial flight.

A = assumed
N = neglected
I = could include
F.S. = Fourier Series

numerical methods to integrate the basic blade element equations.

Results from these calculations are:

a. The calculation of the hub pitch angle required for autorotation using second order Fourier series representation for the airfoil data, i.e., coefficients of lift and drag as functions of angle of attack, has been shown to lack sufficient accuracy. Table 4 lists the results of comparing the second order Fourier series calculations to a high order, accurate representation of the airfoil data.

b. The values of torque, Table 5, calculated for hub pitch variations around states of autorotation using accurate airfoil data representation indicate some of these autorotative states are stable, while others are not. The criterion of stability as employed herein is that if a positive restorative torque accompanies a decrease in the pitch angle, the system tends to be stable. On the other hand a negative torque associated with a decrease in the pitch angle suggests an unstable condition. These arguments apply in reverse for increases in pitch angle.

c. The calculation of thrust using second order Fourier series representation for the airfoil data has been shown to be reasonably valid for a wide range of flight conditions, Table 4, except at the lowest inflow ratio.

d. The assumption of the symmetrical blade section with respect to the transverse axis of the cross-section has been discarded. The use of this assumption resulted in a major error in the Fourier representation of the airfoil data.

The present rotor model will be extended to include lead-lag hinges. The analysis program will then describe the performance of the proposed rotor hub assembly, Task B.2. Equations based on the second order Fourier Series representation of the airfoil data will be developed to permit calculation of autorotation, thrusts, coning angles, etc., developed for the flapping and lead-lag hinge configuration. This additional work, using

TABLE 4 EFFECT OF UNCERTAINTY IN TIP-LOSS FACTOR ON AXIAL THRUST PREDICTIONS

Inputs				Tip-Loss	Axial Thrust			
					High Order		Second Order	
λ	Vel	θ_0	β	$B_{calculated}$	$B_{calc.}$	B=0.97	$B_{calc.}$	B=0.97
1.	453.	.64	.43	.67	124.5	131.4	127.4	134.7
.84	424	.62	.40	.70	127.3	144.1	130.5	148.6
.8	400	.62	.36	.71	121.4	139.5	124.4	144.0
.75	350	.61	.35	.72	101.1	120.3	103.6	124.4
.65	300	.43	.30	.75	90.7	120.4	92.0	123.5
.40	200	.18	.29	.83	68.2	93.6	67.8	94.0
.30	150	.12	.28	.87	54.5	69.4	56.1	72.4
.20	100	.11	.27	.91	42.0	50.3	46.3	54.3
.10	50	.04	.20	.95	55.5	58.5	25.2	26.5

TABLE 5 HUB PITCH ANGLE AND STABILITY PREDICTIONS

λ Inflow Ratio	v Axial Velocity (ft/sec)	Hub Pitch Angle for Autorotation θ_o (Radians) 2nd Order	θ_o High Order	Restoring Torque (ft-lb$_f$) θ_o -.001	θ_o +.001	Stability[1]
.7	349	.901	-.221	.95	-.40	S
		-2.33	2.84	.20	-.17	S
.8	400	.734	-.215	.95	-1.67	S
		-1.40	-.81	-2.86	2.69	U
		1.73	2.36	-.30	5.35	U
		-2.44	2.84	.99	-1.03	S
.9	450	.69	- .212	1.91	-.98	S
		-1.18	- .869	-5.97	.70	U
		1.96	2.29	-4.78	1.97	U
		-2.47	2.94	1.89	-.57	S
1.	500	.677	-.205	2.07	-1.51	S
		-1.05	-.92	-6.76	1.11	U
		2.09	2.24	-2.06	5.9	U
		-2.48	2.86	2.98	- .30	S

(1) S = stable, U = unstable

the rotor with lead-lag hinges, when combined with the results already obtained will provide a realistic insight into the performance of the rigid blade autogyro during descrnt flight conditions.

A comparative payload fraction analysis is scheduled for completion by September 30, 1969. This analysis should permit a realistic evaluation of the possible application of the autogyro as the controlled decelerator for atmosphere entry on Mars and on other planets.

Task B.2. Autogyro Rotor Hub Assembly Design - W.P. Rayfield
Faculty Advisor: Dr. G.N. Sandor

The design of an extremely light weight, high-reliability rotor control hub is essential to the development of a planetary entry and landing autogyro. For the 150-pound earth-weight martian lander, the initial hub allotment of five pounds was the prime optimization goal. The hub capability was to include a rotor speed and thrust control (as a function of the collective blade pitch), a cyclic pitch control, and a coning angle monitor. Lubrication, sterilization, and temperature requirements further restricted the design of most components. A maximum loading of 12-G's was assumed.

Because of the ability of a self-centering, conical, hydrostatic gas bearing to absorb sudden load changes, both axially and horizontally, and its lack of dependence upon liquid lubricants, it has been chosen as the main hub bearing, Fig. 7. It will be constructed of a high strength, light weight alloy such as the Invar. The two smooth shells of the bearing are inverted; the inner is attached to the capsule, the outer to the three blades. Spring actuated, teflon-encased ball bearings provide a backup system for this critical component. Similar solid lubricant bearings carry any short duration reversal loads. In an attempt to extend the life of the hub bearing, an adaptation of a conical vibration-induced squeeze-film bearing proved to be the only marginally feasible due to the thin Martian atmosphere.

The entire hub assembly can be tilted about a bearing within the capsule to effect a change in the cyclic blade pitch. The stationary cylindrical sheet carries gas feed tubes to supply the hydrostatic gas bearing, and the fluid devices controlling the collective blade pitch.

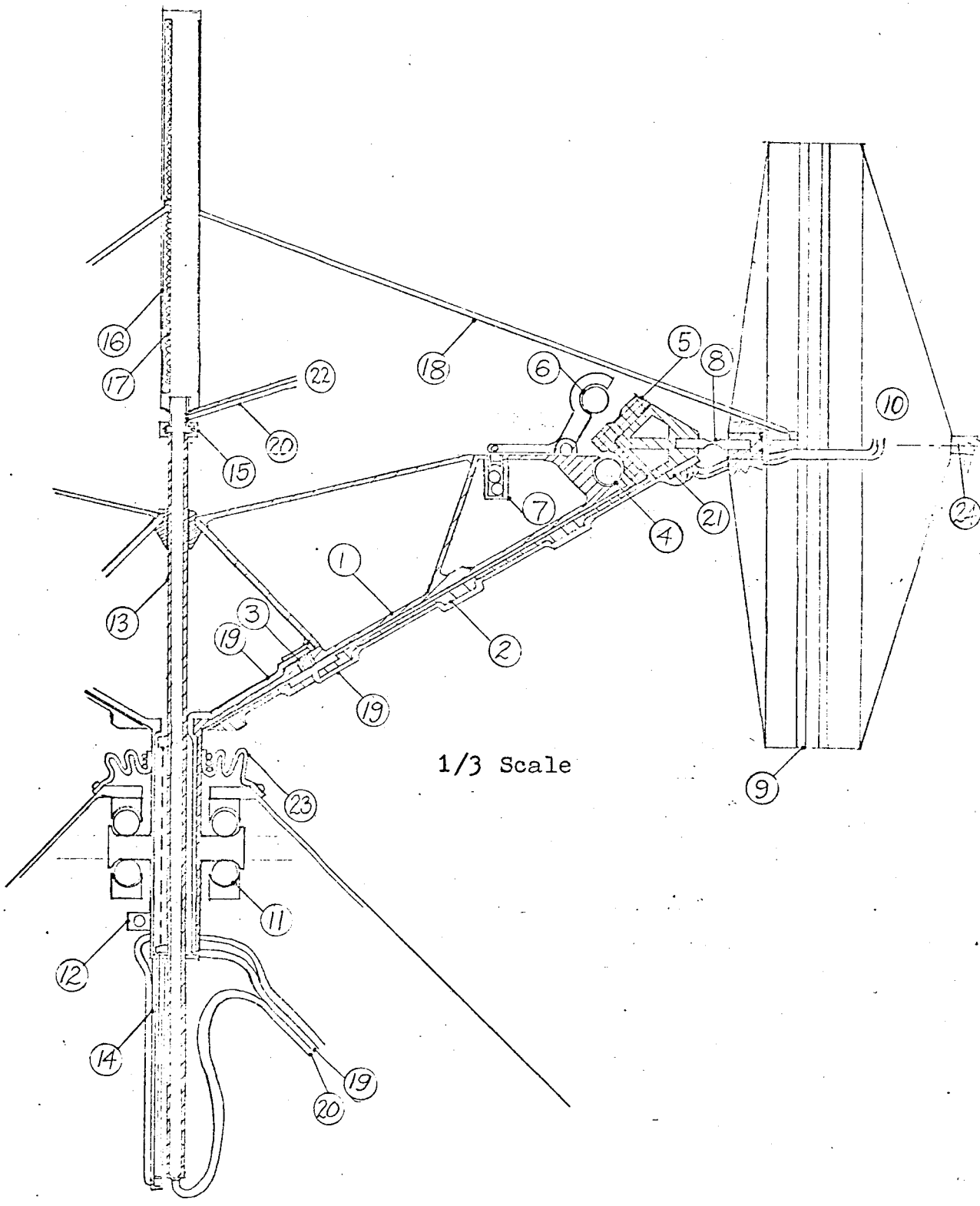

Fig. 7. Details of Proposed Rotor Hub Assembly

Table 1. Legend for Figure

1. Hydrostatic gas bearing - inner cone structure
2. Outer cone structure
3. Porous gas resistor
4. Reversal bearing
5. Nylon roller surface
6. Back-up bearing
7. Rolamite force generator
8. Polypropylene flapping hinge (axial view)
9. Polystyrene lead-lag hinge (side view)
10. Mounting area for collective pitch control mechanism
11. Cyclic pitch control, hub-tilt bearing
12. Hub tilt-actuator mount
13. Coning angle indicator rod
14. Indicator tube
15. Swivel seal
16. Ball slot slides - indicator head
17. Averaging spring
18. Indicator spar
19. Collective pitch control - supply pressure tubing
20. Reference pressure tubing
21. Fluidic control element
22. (Tubing out of plane of indicator spar)
23. Capsule flexible pressure seal
24. Blade pitch axis

The coning angle is monitored by a plastic slider-crank linkage; the slide rod is coaxial with the hub bearing and transmits the coning signal to the capsule. To accommodate coning, flapping, and lead-lag blade movement, and to reduce blade bending moments, two mutually perpendicular hinges are provided for each blade. Tested to nearly 1 million flexes under the anticipated load, thermoplastic integral hinges proved feasible, providing light weight, frictionless one-piece component hinges for the 2000 cycles required for this mission.

All elements of the rotor hub have been defined, most design parameters analytically determined, and certain elements tested, Ref. 7. The total weight of the hub assembly has been reduced to eleven pounds, excluding the collective pitch actuator system, Task B.3.

Further development of this design would require high quality, close toleranced fabrication and sophisticated testing procedures.

A final report providing details of the rotor hub design will be issued by September 30, 1969.

Task B.3. Blade Pitch Control System - R. Wepner
Faculty Advisor: Prof. G.N. Sandor

The problems of pitch control and blade support have been investigated. A pitch control unit proved to be feasible and has been designed for the blade support scheme involving two perpendicular plastic hinges, (see Task B.2.). The objective of the task was to design a pitch control system which would receive a fluidic input signal and fluidic power, and convert this into an angle of attack of the three blades (pitch angle). Several criteria were considered. Loadings of three types were considered: friction, inertia, and aerodynamic loading on the blades. The first two proved to be less than 5% of the 3rd, and were neglected.

The aerodynamic loading was unique in that the torque could assume two possible values: 380 in-lb/blade or 76 in-lb/blade. The high value was possible due to the possibility of a freak occurrence during the landing. Since the probability of this event occurring is unknown, the design has been based on both possible eventualities.

The design is shown schematically in Figure 8. The core is a piston-cylinder actuator. The design for the worst case contains the following details: a wall thickness for the actuator of 0.02"; a pressure drop across the piston of 250 psig; a stroke of 5"; and a bore of 2.64".

It should be noted that these figures contain a safety factor of two for the worst case; and a safety factor of 10 for the other case.

To continue with the rest of the system, the piston drives a flexible cable (1500 # test) around three guide wheels which are similar to pulleys. The cable is guided with the aid of three guide wheels.

The pulleys are not friction drives like ordinary pulleys; rather, they are positive control drives. This is achieved by adjusting the actuator stroke to an appropriate value such that the pulley which rotate only 360° during the descent. With this restriction, the cable can be anchored to the pulley. In this way, complete control over the pitch angle can be achieved.

The drive wheels are mounted on flexible shafts. In the design illustrated, the shaft diameter is .635", the weight of the three shafts combined is 1.4 lbs, and the length of each is approximately 8" from hub to blade. These dimensions are based on flexible shafts sold commercially. They have not been manufactured with weight in mind. It is possible that weight can be reduced with lighter materials without significant losses in torque capability.

The inboard end of the shaft is attached to the hub wall with plain and thrust Teflon bearings. In this way, the shaft and the drive pulley are secured to the hub. The shaft comes outboard and is threaded through the hinge structure. At the hinge segment beyond the second (lead-lag) hinge, the shaft is attached with thrust and plain bearings once again. The shafts continue through this second set of bearings to the blade itself, where it is rigidly attached.

A pitch angle indicator is stationed along the travel of the cable. This is a small piston-cylinder device which will tap off the actual pitch angle and feed it to the control network as a feedback input.

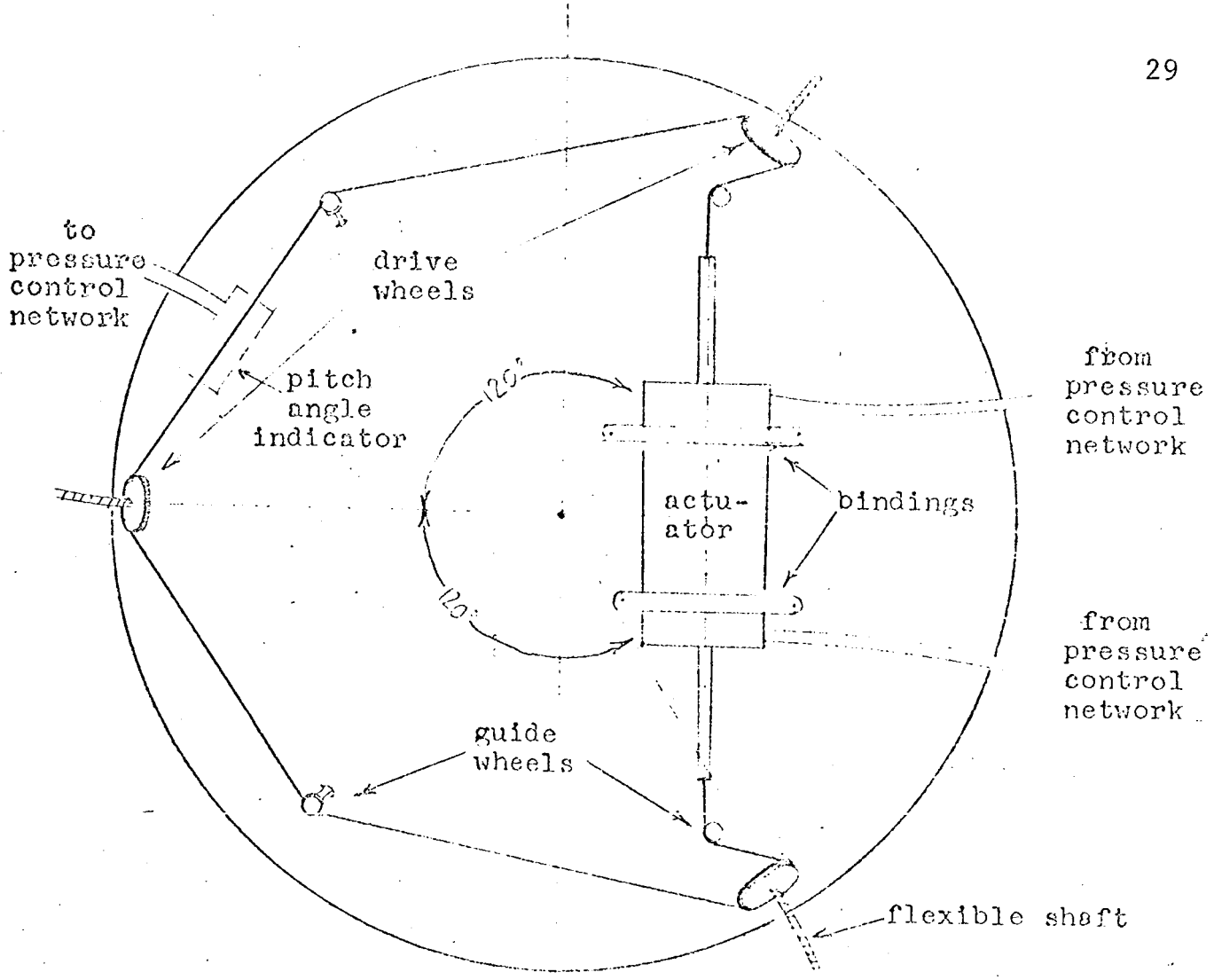

BOTTOM VIEW

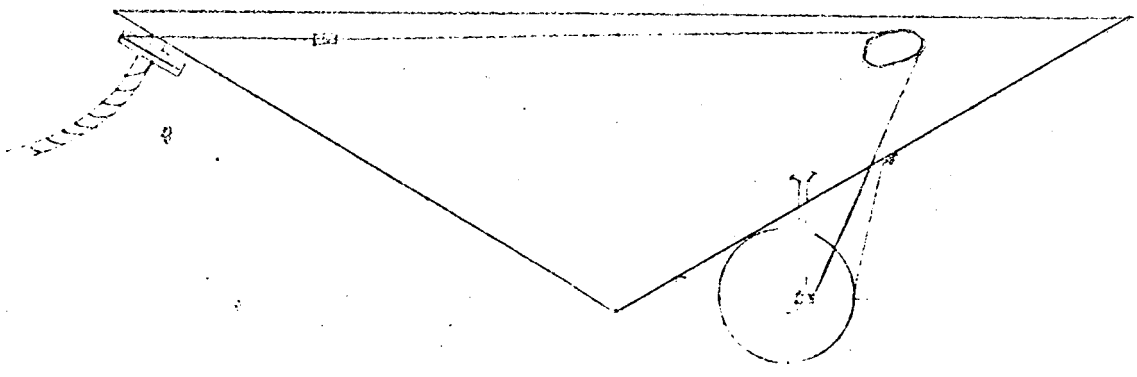

FRONT VIEW

FIGURE 8 Pitch Control System Schematic
(Scale: 1/4 size)

The advantage of this system over others considered earlier is, essentially, that it provides coordination of the motion of the three blades. In addition, it provides dependable blade support (flexible hinges) and reduced weight. The total weight of this system will be approximately 2 pounds.

It should be noted here that the material selected for the actuator cylinder is aluminum. However, the trade-off between weight and strength was such that a heavy material such as steel can be used also.

In all cases, the design around the worst case contains a safety factor of about 2. The other case (loading = 380 in-lb/blade) is overdesigned by a factor of five.

The choice of pressure drops and cylinder diameters is a trade-off between reduced weight (i.e. small cylinder) versus smaller pressure supplies (i.e. large piston; large cylinder). The design chosen was based on space considerations on the hub since the entire system is mounted on the outside conical surface of the hub.

The drive pulley radius is 0.795". This is dictated by the stroke of the actuator, which is constrained by limitations on the pitch angle indicator.

As mentioned above, the development of the pitch control unit is complete and is reported in Ref. 8. More exact data concerning the aerodynamic loading is required before a final design can be made.

Task B.4. Inflatable Blade Design and Fabrication -
J.P. Sadler
Faculty Advisor: Prof. G.N. Sandor

Plastic inflatable blades are presently being considered for use in a Mars landing by autogyro. Lightweight, flexible blades are necessitated by the space and weight restrictions on the landing capsule.

The past period has been devoted to the study of blade design and fabrication. The blade consists of fourteen pressure-tight cylindrical spars of various diameters, an outer skin, and end plugs, Fig. 9. The cylinders are arranged in such a fashion as to approximate a NACA 0012 airfoil section on inflation. The cylinder and outer skin material is a 2 mil or 3 mil thickness of DuPond Kapton Film (a polyimide film base

NON-TAPERED BLADE END

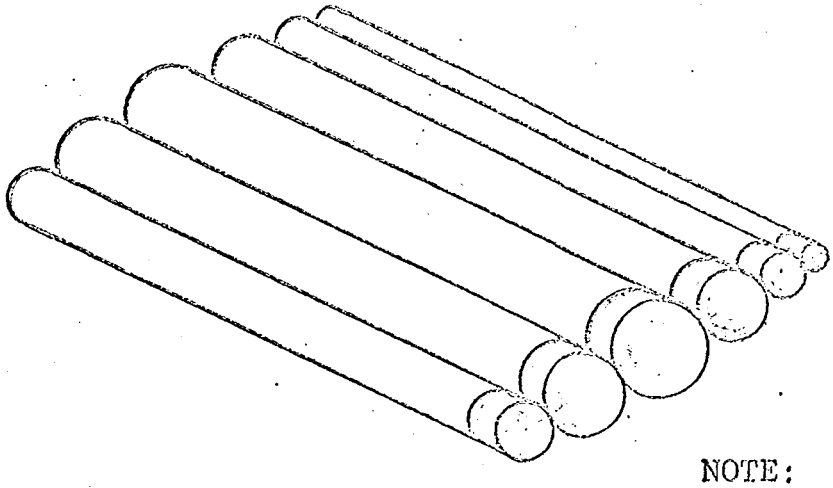

NOTE: The Actual Blade Design Consists of 14 Cylinders.

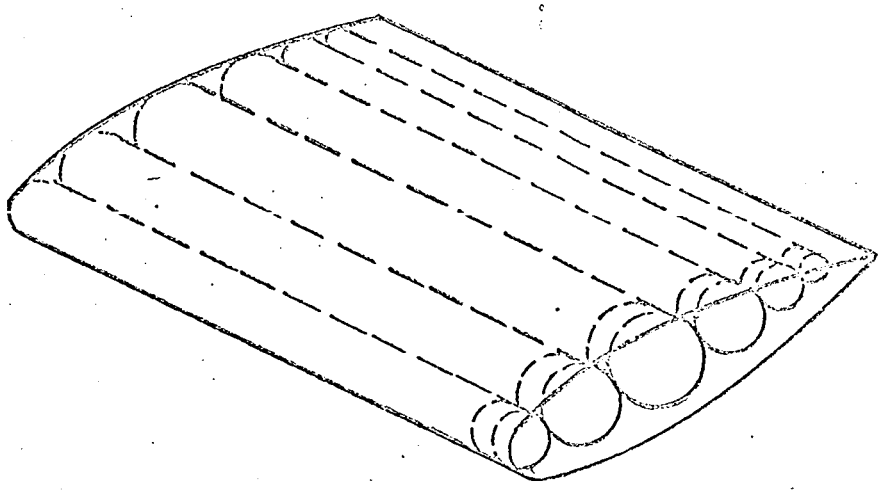

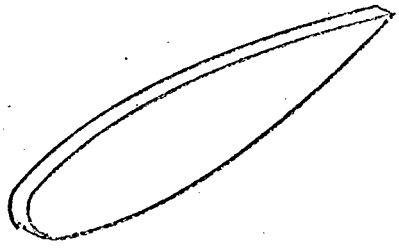

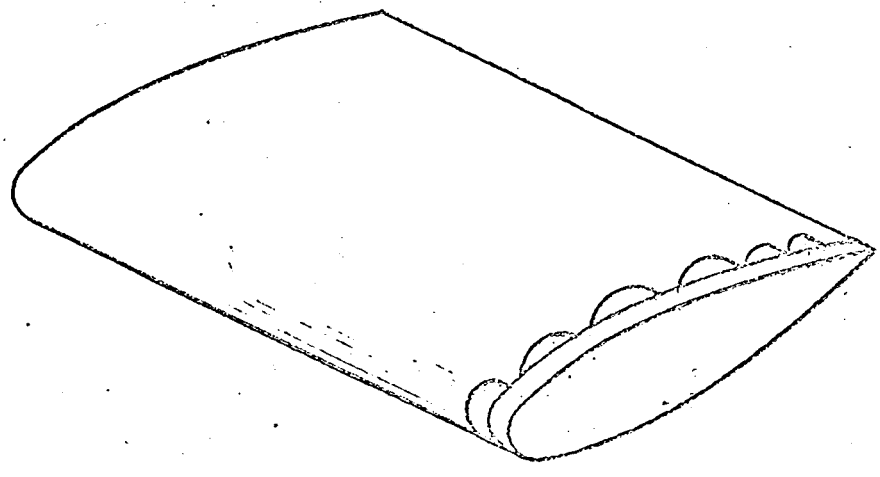

FIGURE 9

with a coating of Teflon FEP fluorocarbon resin). The end plugs are solid Teflon FEP. The use of Teflon, a thermoplastic, permits heat sealing to be used for all fabrication processes. The optimum heat sealing range is 600 - 650°F with a sealing time of 0.5 sec.

Using helium as the inflation gas and 2 mil film, the weight of a 20 ft. blade is 5.6 lbs, almost 2 lbs. above the preliminary estimate. Details are provided in Ref. 9.

Future steps in this area would be actual blade model construction and tests, and a continuation of analytical treatments including factors not present in the cantilever case, such as centrifugal force effects.

Task C. Surface Navigation and Path Control

Task C.1. Long Range Path Selection - R.J. Mancini
Faculty Advisor: Prof. D.K. Frederick

A long range path selection system is to be specified for a roving Martian vehicle. This system will acquire and process measurements of the major terrain features in order to make a decision on a general path to travel to a predetermined mission site, and has been divided into the following four functional areas:

1. Terrain Data Acquisition
2. Terrain Data Processing
3. Terrain Model Generation
4. Path Selection

The calculation of a set of indices was proposed to permit quantitative characterization of pertinent terrain features using measurements of azimuth and elevation angles and range (area 2) was proposed in Ref. 10. Three methods of terrain modeling (area 3) using various combinations of these methods on simulated and actual terrain data has been initiated. A brief description of the three methods follows:

1. Relative Altitude Method

This is the crudest of the three methods under consideration since it does not try to mathematically recreate terrain features (i.e. slopes) and thus should not require high accuracy of the

terrain sensor measurements.

It consists of the following three indices:

(a) Discontinuity Index: The purpose of this index is to sense regions that are hidden in range for a small increment in elevation angle, with azimuth held constant. Figure 10 illustrates the application of this index.

(b) Vertical Index: This index senses a "steep" slope by comparing successive range values along an azimuth direction. Figure 11 illustrates its application.

(c) Relative Altitude Index: This index determines if terrain is high or low relative to the vehicle. The rationale for such a criterion is that a significant change in the height of the terrain may require a steep slope, as indicated in Figure 12. A limitation of this test is that it may miss finding obstacles or may incorrectly label relatively safe high or low terrain as an obstacle.

2. Slope Method

This method attempts to make a more refined estimate of the passability of the terrain by making a discrete approximation to the slope of terrain. In addition to the discontinuity index (1.a), it consists of a slope index.

(a) Slope Index: As indicated in Fig. 13, the slope of the terrain can be approximated by the relationship

$$S = \frac{R_{i+1}\beta_{i+1} - R_i\beta_i}{R_{i+1} - R_i}$$

where R_i and β_i are the range and elevation angle. The index would be satisified if $|S| < \tan 10^o$, for example.

3. Gradient Method

The second index in this method seeks to find a terrain obstacle in an area of terrain by calculating a linear approximation to the magnitude of the gradient (steepest slope in any direction)

of the terrain feature. The Gradient Method overcomes a limitation of the slope method above. Consider the following: "The slope along a profile of the terrain is only less than or equal to the steepest slope that the vehicle could encounter on the terrain feature. The slope method calculates the slope along a profile and thus may miss some actual obstacles". The Gradient Method is the most sophisticated of the methods proposed and should be the most sensitive to sensor measurement errors. This method is similar to the slope method with the exception that an approximation to the gradient rather than just the slope in the direction of travel is included.

(a) Gradient Index: This index seeks a linear approximation to the gradient of a terrain feature by computing the "in-path" slope (constant azimuth) and the "cross-path" slope (constant elevation angle). Then the gradient index is defined to be the square root of the sum of the squares of these slopes and must be less than some preset level for that portion of the terrain to be designated as passable.

The terrain modeling methods described above were programmed on a WANG 370 Series Calculator (a programmable electronic desk calculator) in order to provide a means of simulating the operation of the modeling methods.

For example, using terrain data from a Geological Survey map with 4 milliradian increments in elevation angle to obtain the discrete sensor data, the following results were obtained for one assumed location of the vehicle: (i) the gradient and slope method each found 70% of the passable terrain in a sector of 35 degrees. (ii) in azimuth, the relative altitude method found 57% of the passable terrain. As the size of the angular increment in in elevation angle increased, fewer discrete data points were available and the effectiveness of all three methods decreased, asymptotically approaching the same effectiveness value.

During the next period, sectors of terrain as viewed from different vantage points will be used to generalize the results of this investigation. The selected observations in the preceeding paragraph are

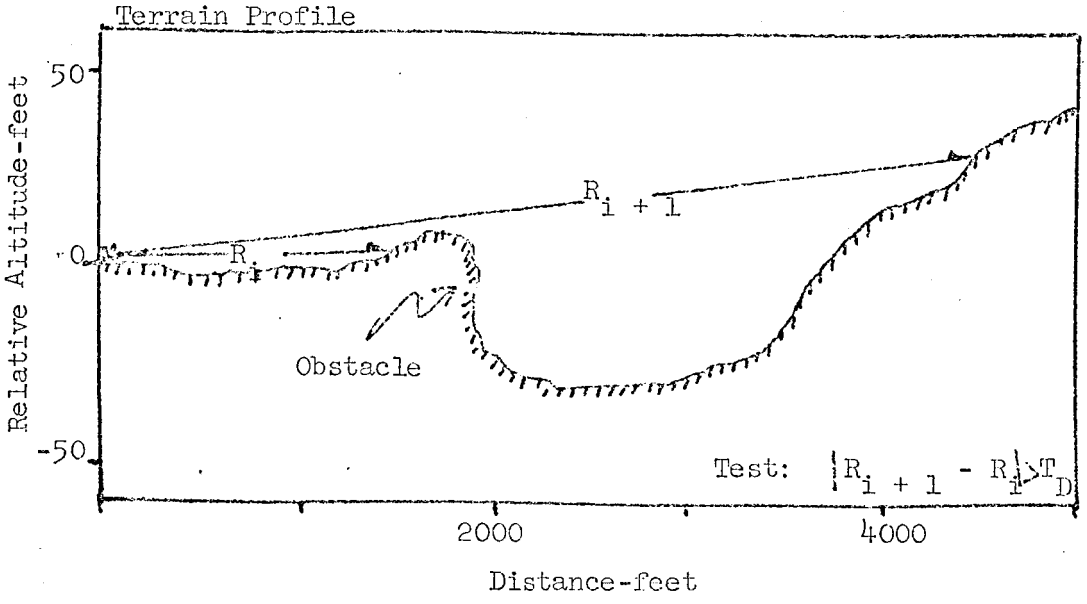

Figure 10. Illustration of Discontinuity Index

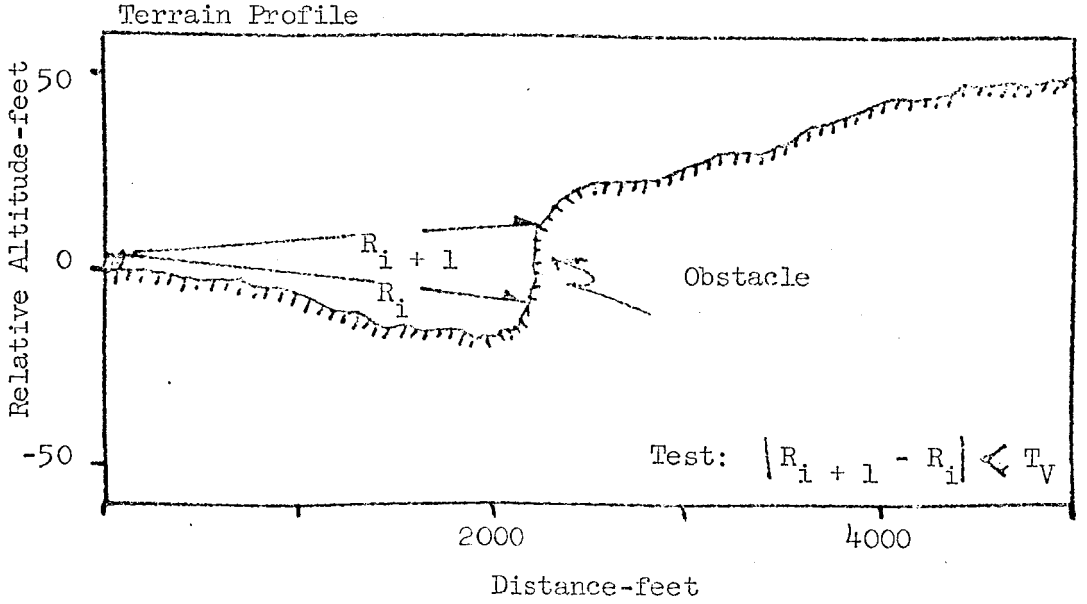

Figure 11. Illustration of Vertical Index

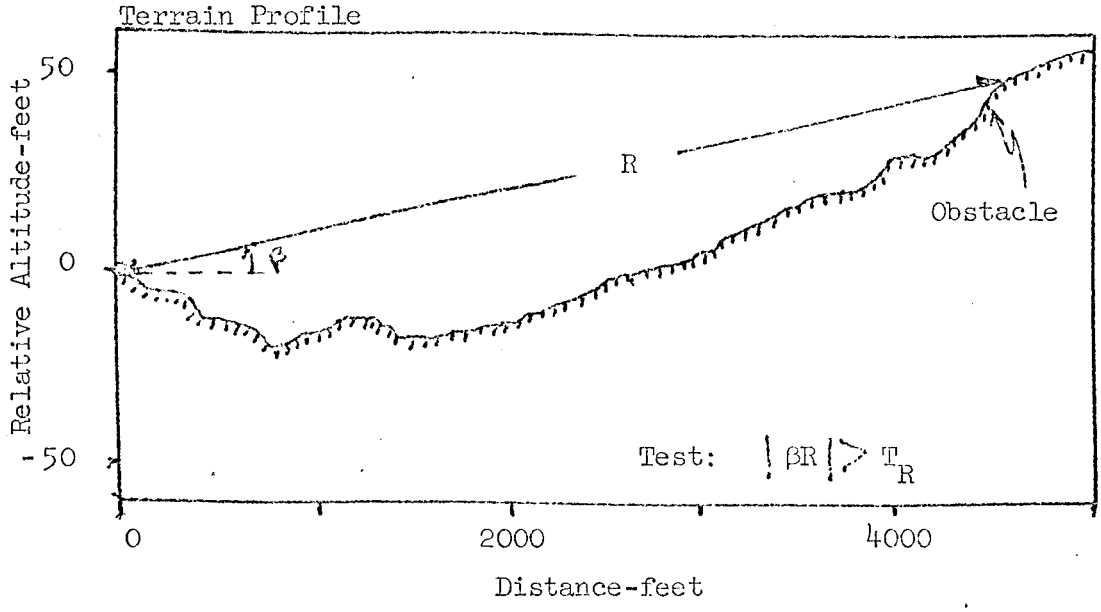

Figure 12. Illustration of Relative Altitude Index

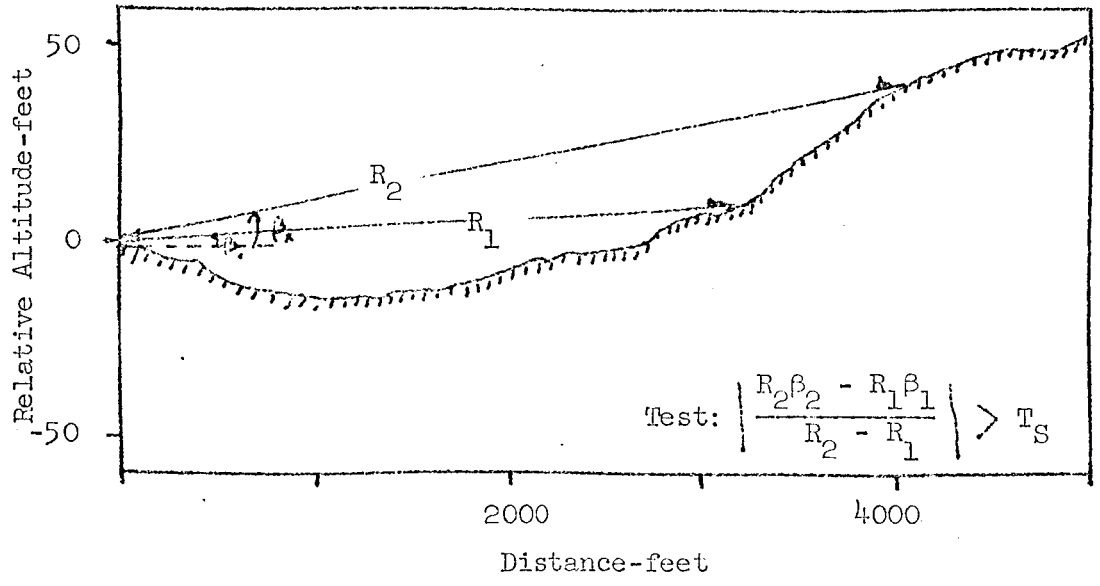

Figure 13. Illustration of Slope Index

typical of the type of analysis that is to be made. Some of the results expected from this phase of the study are:

1. Quantitative measure of the effectiveness of the terrain modeling methods to find safe areas of travel on certain types of terrain.

2. A measure of the effect on the modeling methods of using finer (or coarser) angular increments to obtain sensor information.

3. An indication of the range resolution needed to perform selected modeling tasks.

Task C.2. Short Range Obstacle Detection System -
G. LaBarbera
Faculty Advisor: Prof. D. Frederick

The goal of a short range obstacle detection system is to alert the vehicle to the presence of obstacles which it cannot negotiate directly and to initiate manuevers that will avoid such obstacles. This task is specifically directed at the design and evaluation of a device to detect positive or protuberance type obstacles.

In brief, this system takes advantage of the following concept. The sharpness of the image of an object depends on how well focus has been obtained. As the image passes in or out of focus, the light forming the image is either well concentrated or is dispersed. Since a non-linear photoresistive detector (CdS cell) will provide a resistive change which is related to the detailed pattern of incident light, it is conceivable that this output can be related to the distance at which the obstacle is located.

The investigation of this focusing method of obstacle detecting, utilizing a CdS cell as the focus detector and a single lens, has been concluded. Results have ranged from encouraging to completely negative.

As discussed in greater detail in Ref. 10, the focusing method of rangefinding shows much promise due to its inherent simplicity and ruggedness. The method can and will work if a suitable focus-detecting method can be found.

Unfortunately, the CdS cells investigated here

have not proven satisfactory. Under certain conditions, (high contrast line targets) they can detect focus far better than the human eye. Results with a Ronchi grating line target are equivalent to the human eye aided by 30X magnification. Resistance changes amounted to about 5-10%. However, when presented with a continuous half-tone of arbitrary contrast distribution, the cells would not respond in a positive fashion. Tests were run on a topographical terrain modeling table using various sands and rock of approximately 4 to 6 inch size. Distances involved were about forty to fifty inches.

Here it must be stated that one important variable, namely cell structure, was not under direct control. While geometry could be controlled the material constituency of the cells or the processes by which they were manufactured could not be controlled. It is felt, however, that the type 3 CdS material used in these cells is very representative of modern, panchromatic sulphides.

The failure of CdS cells as a focus detector should not detract from the optical focusing method. This system remains the only one of several considered that becomes more accurate as the range shortens. Possibly the solid state vidicon mentioned in Ref. 11 could be the focus detector that makes the system practical. Here the analysis of the high frequency content of the output is used to determine whether or not the image is in focus. The field of view problem can be solved using a gimbaled mirror in front of the optics.

Details of this study of the use of non-linear photoresistive cells for obstacle detection are provided in Ref. 12 which is to be issued shortly.

Task D. Vehicle Dynamics and Attitude Control

Task D.1. Dynamics of a Two-Segmented Vehicle -

J.A. Hudock
Faculty Advisor: Prof. E.J. Smith

The Martian roving vehicle will undoubtedly require some form of passive suspension. This need for passive suspension comes from present theories about the make-up of the Martian surface. The terrain of Mars is expected to be somewhat similar to that of the moon in that the landscape is dotted with craters and rocks of various sizes. The vehicle should be capable of negotiating

many of the smaller obstacles without damage to onboard instruments and systems, as well as the vehicle itself.

Protection of the vehicle and its equipment from the effects of an uneven terrain can be provided by a passive suspension system, which due to its passive nature, will consume no power from the vehicle's limited supply. The passive suspension system would, if properly designed, reduce the effects of shock and impulse forces acting on the vehicle from uneven terrain and reduce the amplitude and duration of transient oscillations of the vehicle caused by the terrain.

Preliminary studies of a passive suspension system for a single segment vehicle has been reported in Ref. 11. This suspension was concerned primarily with minimizing the oscillations induced by an uneven terrain. The single segment vehicle was limited to three degrees of freedom, pitch heave and roll and the equations of motion used in the analysis were linearized about a nominal equilibrium point.

The single segment vehicle had one major drawback in that the heave and pitch motions of the vehicle were required to have natural frequencies of motion in excess of 2.5 radians per second. The studies made by General Motors and Bendix recommended that vehicle motion have natural frequencies between 2.0 and 1.0 radians per second and dampening factors between 0.63 and 0.90, or slightly underdamped. The single segment vehicle required such a high frequency of motion for the heave and pitch channels to keep the roll motion stable. Even under these conditions roll channel motion was very lightly damped.

A two-segment vehicle with a flexible connection between segments has an additional variable in the flexibility of the coupling. This flexibility provides an added stability to vehicle motion not found in a single segment vehicle. The model used in this investigation is shown in Figure 14. Basically the vehicle consists of two rectangular segments connected by an elastic rod and mounted upon a passive, suspension modeled as parallel spring and dashpot arrangements.

The equations of motion for the two segment vehicle were developed for the heave pitch and roll motion of each segment. These equations were further simplified by restricting motion to small deviations from a nominal rest point and resulting in a set of linear

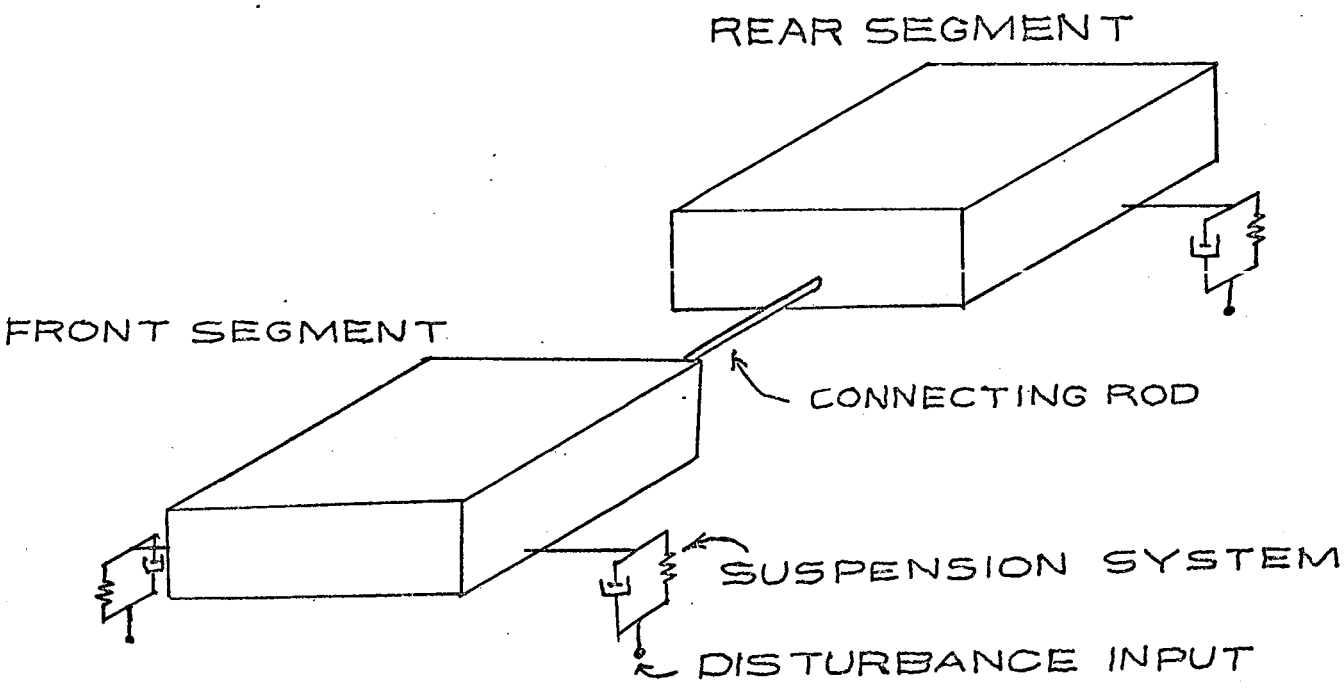

Figure 14. Two-Segment Model

differential equations for vehicle motion. The form of the equations of motion for each segment is similar to those reported in Ref. 11 with additional terms representing the coupling between segments due to the connecting rod.

The analysis of the two-segment model differed from that made on the single segment vehicle in that it was made from a frequency domain analysis rather than a time domain analog simulation. The frequency domain uses such techniques as system transfer functions and root locus plots to determine the natural frequencies and dampening factors for the channels of motion of the vehicle model.

The results of studies made by General Motors and Bendix on several vehicle configurations were used to provide a set of system specifications to limit the vehicle response in all channels of motion to be between 2.0 and 1.0 radians per second on natural frequency of oscillation and with dampening factor of 0.63 to 0.90. A vehicle whose response meets the specifications will exhibit satisfactory performance. By satisfactory performance is meant that the response of the vehicle to terrain disturbances will be within tolerable limits for induced oscillations and the effects of shock and impulse forces.

The study of the two-segment vehicle has shown that the suspension parameters and the elasticity determine, to a large extent, the vehicle response. By choosing vehicle dimensions in line with those used in Ref. 11 and observing the effect that the various suspension parameters had on vehicle response it was possible to choose parameters in the suspension system to provide an acceptable vehicle response. The parameters for the elasticity and viscous dampening of the suspension system were somewhat greater than those reported for the single segment vehicle. This results in a more sluggish response to disturbances causing lower accelerations on the vehicle performance while still having a relatively rapid settling time. The flexible connecting rod served to uncouple the motion of the front segment from the rear segment. Its greatest effect was in the roll channel motion of both segments. By fixing a suitable value for the connecting rod elasticity, the value being determined by the restrictions on the roll channel frequency response, the roll motion can be kept within the system specifications.

The two-segment vehicle has a decided advantage over a single-segment vehicle in that its response to disturbance inputs can be controlled by a passive suspension system. This is due to the vehicle added flexibility in conforming to the contour of the terrain both while the vehicle is stationary and in motion. The addition of a third segment and an additional flexible coupling may result in an even superior vehicle design. A three segment vehicle would extend even further the overall flexibility of the vehicle response. This vehicle response would be with regard to both induced oscillations as well as induced accelerations caused by terrain variations.

Reference 13, scheduled to be issued in the near future, provides details of this investigation.

Task D.2. Attitude Detector Systems - A. Himmel, J. Jendro, J. Mleziva, N. Pinchuk
Faculty Advisor: Prof. E.J. Smith

The purpose of this task was to design an attitude sensing system for the Mars rover vehicle. Three different types of instrumentation were to be investigated. These systems included Two-Degree-of-Freedom gyro system, a Pendulous-Two-Degree-of-Freedom gyro system and a Rate gyro system. The entire group was composed of four people, two of which worked on the pendulous system and one each worked on the gyro systems. The utility of the system was envisioned to provide both a basis for navigation and a mechanism for avoiding non-negotiable terrain.

It was anticipated that this vehicle may experience large displacements. Because of this, the system therefore was analyzed without the aid of small angle approximations.

The first approach to this problem was to attack the dynamics of each device. Upon investigation of the input-output relationships of the several systems, it was found that each system had one common problem. This problem was that the outputs of the attitude systems did not uniquely define the orientation of the vehicle. In view of the seriousness of this problem, it was decided to delay the dynamic studies and turn the major effort to finding a unique vehicle orientation description in terms of the system sensor outputs.

A review of the literature revealed very little applicable material because of the small angle approximations. Since the large angle requirement was considered essential, a fundamental mathematical analysis* was undertaken and a transform relating the output of the two-degree-of-freedom gyro and the Euler angles was obtained.

The pivotal point in the development of this transform is the implementation of a little known angular momentum theorem. This theorem, in effect, allows the representation of a sequence of rotation, about the Euler axes by the same sequence in reverse and about the three original axes. Combining this theorem with appropriate matrix manipulations, a relationship is derived which allowed the definition of the vehicle orientation in terms of the sensor outputs without ambiguity.

The angular momentum equation referred to above in matrix form is:

$$J_{\psi}'' \, T_{\theta}' \, L_{\phi} = L_{\phi} \, T_{\theta} \, J_{\psi}$$

Where the primes indicate the rotations about the new (rotated) axes.

The left side of this expression represents an Euler sequence of rotations:

L_{ϕ} is a rotation about the original z axis through an angle ϕ.

T_{θ}' is a rotation about the daughter x axis (the x' axis) through an angle .

J_{ψ}'' is a rotation about the granddaughter y axis (y'' axis) through an angle .

The z, x', and y'' axes are Euler axes and are not orthogonal. Physically, the left hand side of the

---

* Prof. R.M. Lichtenstein of the Rensselaer Department of Physics provided the basic approach to this problem and his assistance is gratefully acknowledged.

theorem expression represents a sequence of rotations in the order ϕ, θ, ψ about the three Euler axes.

The right side of the theorem represents three rotations about the original x, y, and z axes, $[L_\phi, T_\theta, J_\psi]$ together area rotation sequence through the angles ψ, θ, and ϕ about the three orthogonal axes x, y, and z.

With a gimalled device, Fig. 15, $\phi = 0$ and consequently $L_\phi = 1$. Therefore:

$$J''_\psi \, T'_\theta \, (1) = (1) \, T_\theta \, J_\psi \qquad \text{(D-1)}$$

The next step is to define a unique ROTATION matrix, R, which describes the fictitious axes in terms of an inertial axes. The operation of R on the space-fixed inertial axes results in:

$$\underline{i}_{v_{old}} \triangleq R \underline{i}_s$$

which can be easily expanded to the three dimensions.

The rotations about the three fictitious axes are now defined in terms of the rotations about the inertial coordinate axes.

$$J_\psi = R \, S_\psi \, R^{-1} \qquad T_\theta = R \, V_\theta \, R^{-1} \qquad \text{(D-2)}$$

where S_ψ and V_θ are rotations about the space-fixed axes.

Substitution into the original theorem statement yields:

$$\underline{j}_{new} = R \, V_\theta \, S_\psi \, jg \qquad \text{(D-3)}$$

Three devices are utilized. Each device has an

inertial axis orthogonal to the other two:

$$\underline{j}_{new} \triangleq \underline{i}_g \quad \text{device \#1} \tag{D-4a}$$

$$\underline{j}_{new} \triangleq \underline{j}_g \quad \text{device \#2} \tag{D-4b}$$

$$\underline{j}_{new} \triangleq \underline{k}_g \quad \text{device \#3} \tag{D-4c}$$

Applying the above equations and (D-3) to each of the three devices:

$$R^{-1}(1) = V_{\theta_1} S_{\psi_1} \underline{j}_g \underline{i}_j + V_{\theta_2} S_{\psi_2} \underline{j}_g + V_{\theta_3} S_{\psi_3} \underline{j}_g \underline{k}_g \tag{D-5}$$

Using the proper substitutions, for example S

$$S_{\psi} = \begin{vmatrix} (\cos\psi) & -(\sin\psi) & 0 \\ (\sin\psi) & (\cos\psi) & 0 \\ 0 & 0 & 1 \end{vmatrix}$$

and noting that $R^{-1} = R^T$, the matrix "R" is obtained:

$$R = \begin{vmatrix} (-\cos\theta_1 & \sin\psi_1) & (\cos\psi_1) & (\sin\psi_1 & \sin\theta_1) \\ (-\cos\theta_2 & \sin\psi_2) & (\cos\psi_2) & (\sin\psi_2 & \sin\theta_2) \\ (-\cos\theta_3 & \sin\psi_3) & (\cos\psi_3) & (\sin\psi_3 & \sin\theta_3) \end{vmatrix} \tag{D-6}$$

It is intuitively obvious from (D-4) that

$$\underline{k}_g = \underline{i}_g \times \underline{j}_g$$

The significance of this is that the third device is not needed. $\underline{k}_g$ is determined by $\underline{i}_g$ and $\underline{j}_s$.

For a two device system:

$$R = \begin{vmatrix} (-\sin\psi_1 \quad \cos\theta_1)(\cos\psi_1)(\sin\psi_1 \quad \sin\theta_1) \\ (-\sin\psi_2 \quad \cos\theta_2)(\cos\psi_2)(\sin\psi_2 \quad \sin\theta_2) \\ \quad A \qquad\qquad\qquad B \qquad\qquad\qquad C \end{vmatrix} \qquad (D\text{-}7)$$

where

$$A = \cos\psi_1 \sin\psi_2 \sin\theta_2 - \sin\psi_1 \sin\theta_1 \cos\psi_2$$

$$B = \sin\psi_1 \cos\theta_1 \sin\psi_2 \sin\theta_2 - \sin\psi_1 \sin\theta_1 \sin\psi_2 \cos\theta_2$$

$$C = \cos\psi_1 \sin\psi_2 \cos\theta_2 - \sin\psi_1 \cos\theta_1 \cos\psi_2$$

The Euler angles defining the orientation of the vehicle can thus be obtained by comparing this matrix term by term with a rotational matrix generated by an Euler sequence.

This transform proved useful in its application to position devices, which include the gimballed pendulum and two degree of freedom gyros, but because of basic differences in the rate gyro sensor system these relationships do not apply to the latter configuration.

For the appropriate system, this derivation is general enough to be used as originally desired, both for navigation and for avoiding non-negotiable terrain, and no small angle approximations are employed.

Further study should be directed to the rate gyro system problem to dynamic analysis of each system, and to accounting for the rotation of the planet for the gyro systems.

The aim of this task was to develop a method for determining the vertical reference during a roving excursion on the surface of Mars. This study has investigated a more general case; not only the vertical reference but also the attitude of the vehicle with respect to inertial space.

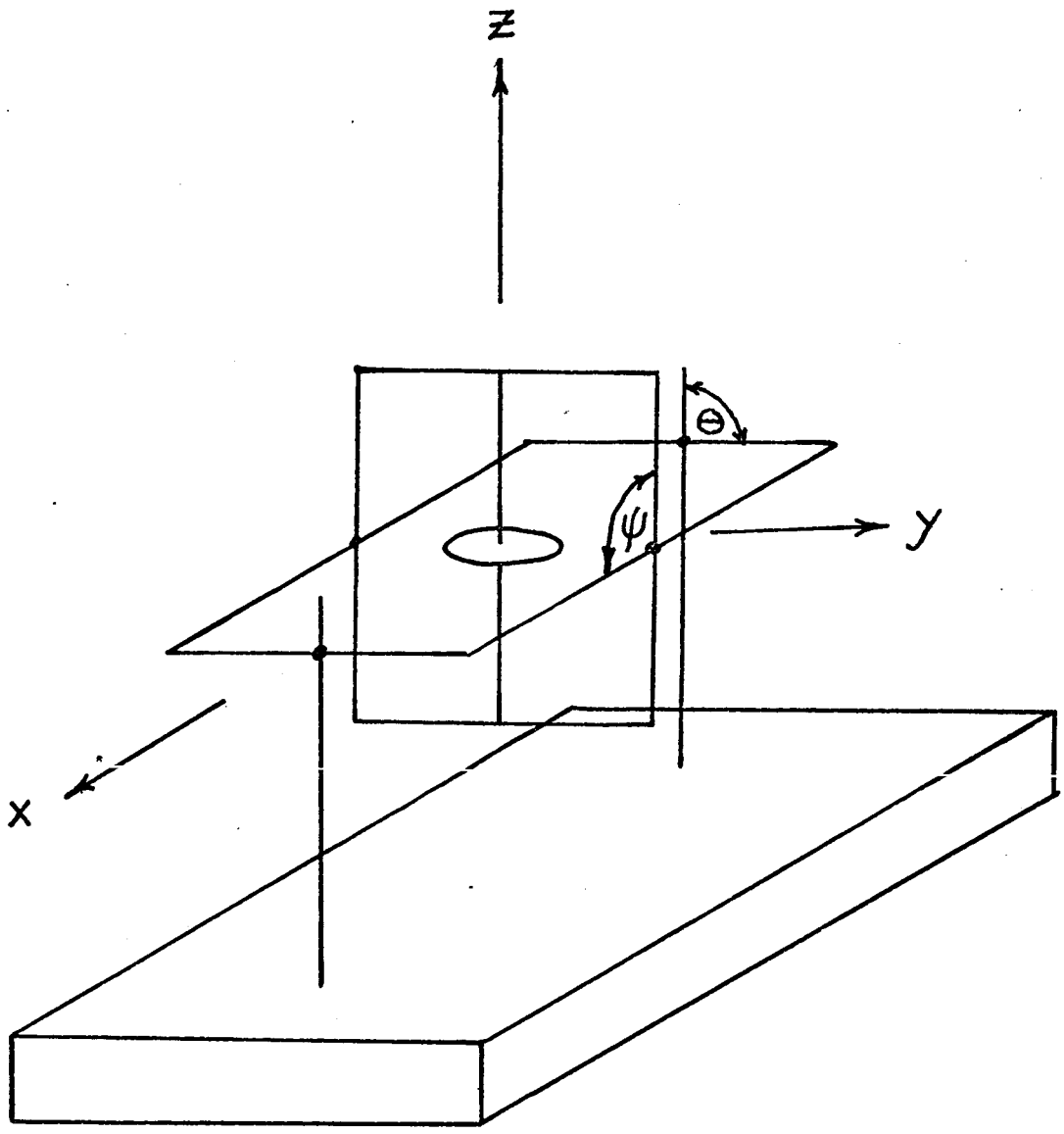

FIGURE 15. Two-Degree of Freedom Gyroscope

The transformation shown in (D-6) and (D-7) allows the vehicle's orientation to be unambiguously defined by the gimbal angle outputs of either three gyro or two gyro systems. Since the gyro provides a space fixed reference and since the transformations allow large angles, the end results of this project has been a development of a strapped down gyro system which, when set at an inertial reference position, will determine the orientation of the vehicle with respect to the reference; that is, it provides the same information as an inertial platform without actually using an inertial platform. It thus provides the basis for navigation and a mechanism for avoiding non-negotiable terrain. The attitude detection system may utilize as few as two-degree-of-freedom gyros and its performance will be independent of the presence of a gravity reference.

Additional details of the investigations described above can be found in Ref. 14, 15, 16 and 17.

Task E. Chromatographic Systems Analysis

One important phase of the initial missions to Mars is the search for organic matter and living organisms on the martian surface. The present concept for attaining this objective consists of subjecting samples of the atmosphere and surface matter to certain chemical and biologically-related reactions and thereafter analyzing the products produced, probably in a combination gas chromatograph/mass spectrometer. It is the objective of this task to generate fundamental engineering design techniques and system concepts for use in optimizing the design of such a chromatographic separation system.

Because of the variety of mixtures to be separated and the complexity of the separating process, a system analysis based on the mathematical simulation of the chromatograph is being undertaken. This technique will use mathematical models, which will incorporate fundamental parameters evaluated from reported experiments, to explore various concepts to direct further experimental research.

A mathematical model of the chromatographic column, based on the unsteady state mass transport of a single chemical species in a carrier gas/adsorbent system was derived earlier, Ref. 18:

$$\left(\frac{\partial y}{\partial \theta}\right) = -\frac{1}{1-y}\left(\frac{\partial y}{\partial z}\right) + \frac{1}{Pe}\left(\frac{\partial^2 y}{\partial z^2}\right) - N_{tOG}\,(y - y^*) \quad \text{(gas phase)}$$

$$\frac{1}{R_o} \frac{\partial x_L}{\partial \theta} = N_{tOG} \quad (y - y^*) \qquad \text{(adsorbent phase)}$$

$$y^* = m \quad x_L \qquad \text{(adsorption thermodynamics)}$$

in which

y = gas composition

y^* = gas composition in equilibrium with adsorbent phase

z = position in column

θ = time

x_L = composition in adsorbent phase

R_o = ratio of amount of gas to amount of adsorbent in column

m = adsorption constant

Pe = column parameter related to axial diffusion of the species

N_{tOG} = column parameter related to the approach to equilibrium adsorption

The second derivative appearing in the gas phase equation represents the gaseous diffusion of the adsorbing compound in the direction of carrier gas flow. In the initial studies, Ref. 18, this term was neglected, because in many situations, especially when the diameter/length ratio of the column is small, it is not of prime importance. The solution to the chromatograph equations, assuming the sample was injected as an impulse, was obtained, Ref. 18, and was compared to an experimental chromatogram for pentane, Fig. 16. This model, designated as the "first-order model" exhibited the basic characteristics of the experimental data, although it failed significantly in predicting peak spreading. Because a reasonably accurate model is required in system evaluations, new studies were undertaken.

It was believed that the spreading could be attributed to either the diffusional effects neglected in the first order model, or to imperfect injection of the samples (injection as opposed to an impulse), or to a combination of

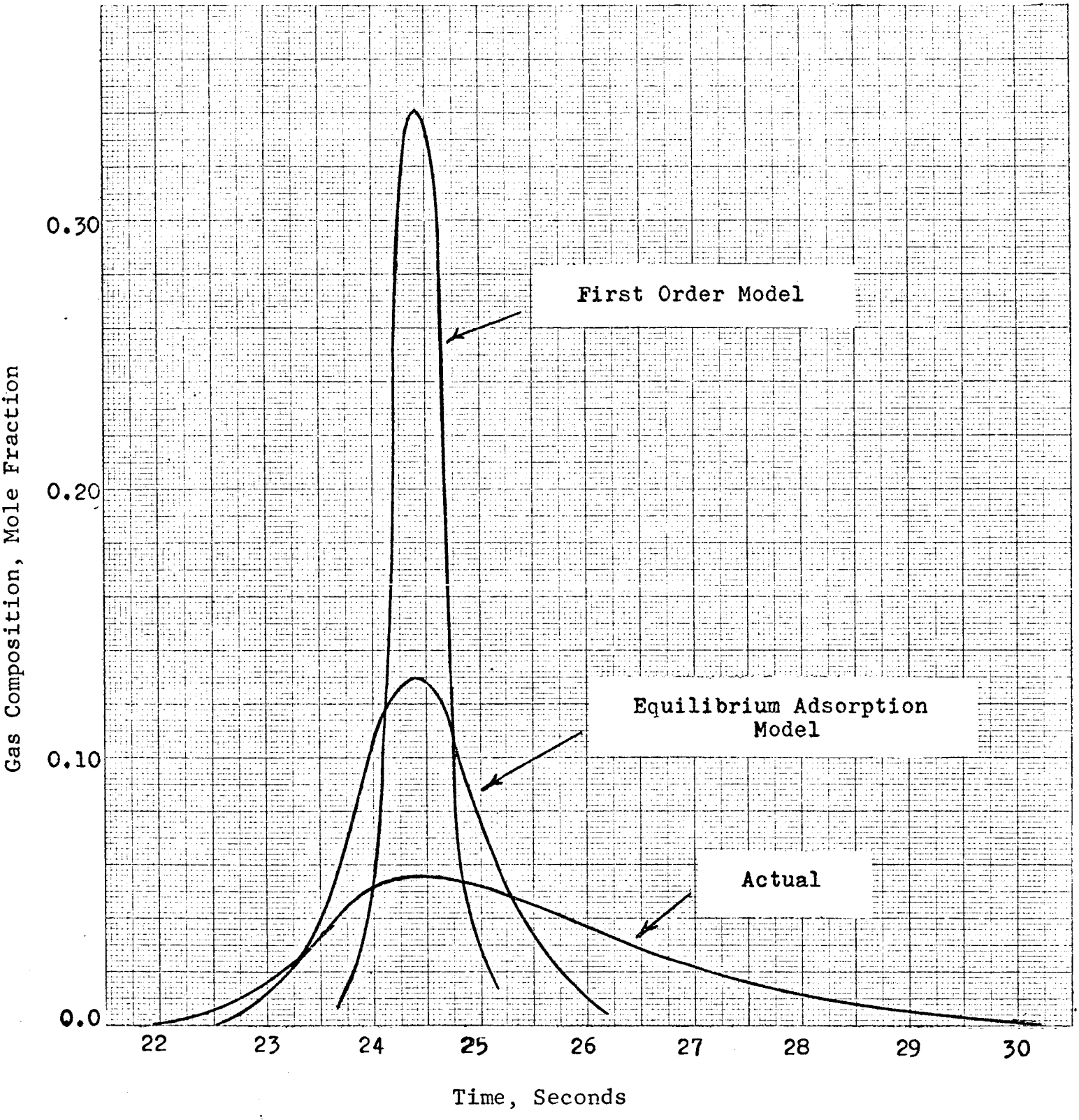

FIGURE 16. Comparison of Two Chromatograph with Pentane Chromatogram

both. These problems were attacked by a three-member team, each of whom pursued specific assignments:

1. Improvement of the mathematical model by considering the second order or diffusional term.

2. Development of methods for predicting the column parameters which appear as constants in the system equations.

3. Investigation of the effect of sample injection time upon the resulting chromatogram.

Task E.1. Second Order Model Analyses - W.A. Voytus
Faculty Advisor: Prof. P.K. Lashmet

The chromatographic equations have not been solved in convenient form. Lapidus and Amundson, Ref. 19, gave a formal solution to the problem in the form of integrals of Green's functions but did not evaluate the solution. Because of the lack of a convenient solution, most work has involved the analysis of the statistical moments, Ref. 21, 21, 22. These time-moments, defined as

$$\bar{\theta} = \frac{\int_0^\infty \theta y \, d\theta}{\int_0^\infty \theta} \quad ; \quad \mu_k = \frac{\int_0^\infty (\theta - \bar{\theta})^k \, y dy}{\int_0^\infty y \, d\theta}$$

and which can be obtained from the transform of the solution to the chromatograph equations have been used to estimate column parameters Pe and N_{tOG} from chromatographic data, but have not been used to characterize the chromatogram from parameter data. The objective of this task was to relate quantitatively the theoretical moments to the chromatogram. Because the moments are relatively simple functions of the column parameters, such relations would be useful for two reasons:

1. The moments could be used to characterize systems for preliminary estimates.

2. The moments results could possibly improve the computational procedures for the Lapidus-Amundson integrals mentioned above.

Because a complete solution to the chromatogram was not in practical form, the equations were solved for the limiting case of equilibrium adsoprtion, Ref. 23.

Mathematically, this implied

$$N_{tOG} \longrightarrow \infty ; \quad (y - y^*) \longrightarrow 0$$

This assumption was not unreasonable because N_{tOG} for practical columns is of the order of 10^4 or more. Because the equilibrium adsorption model represented fairly well the actual pentane chromatogram, Fig. 16, it was believed that results obtained from the moment analysis of the model would be generally applicable.

For the equilibrium adsorption, it was found that the mean time $\bar{\theta}$ was independent of diffusion and could be computed as

$$\bar{\theta} = 1 + (1/m\ R_o)$$

It was further found that the deviation between the chromatogram mean time $\bar{\theta}$ and the time when the maximum composition appeared, θ_{max}, could be correlated with the moments as shown in Fig. 17. The correlating variable Δ was defined as

$$\Delta = (\bar{\theta} - \theta_{max})/\bar{\theta}$$

For the equilibrium adsorption model, the second two moments appearing in the abscissa of the correlation were computed as follows:

$$\mu_2 = 2\bar{\theta}/Pe \ ; \quad \mu_3 = 12\ \bar{\theta}^3/Pe^2$$

This correlation, then, provides a means for estimating the time of peak appearance, knowing only the system parameters and the moments as obtained from the transforms of the system equations.

To estimate the degree of spreading the variance σ^2_{max} about the maximum point was investigated. This variance could be computed from the system moments by

$$\sigma^2_{max} = \mu_2 + (\bar{\theta}\Delta)^2$$

It was found that in the range of $(30 \leq Pe \leq 1000)$ and

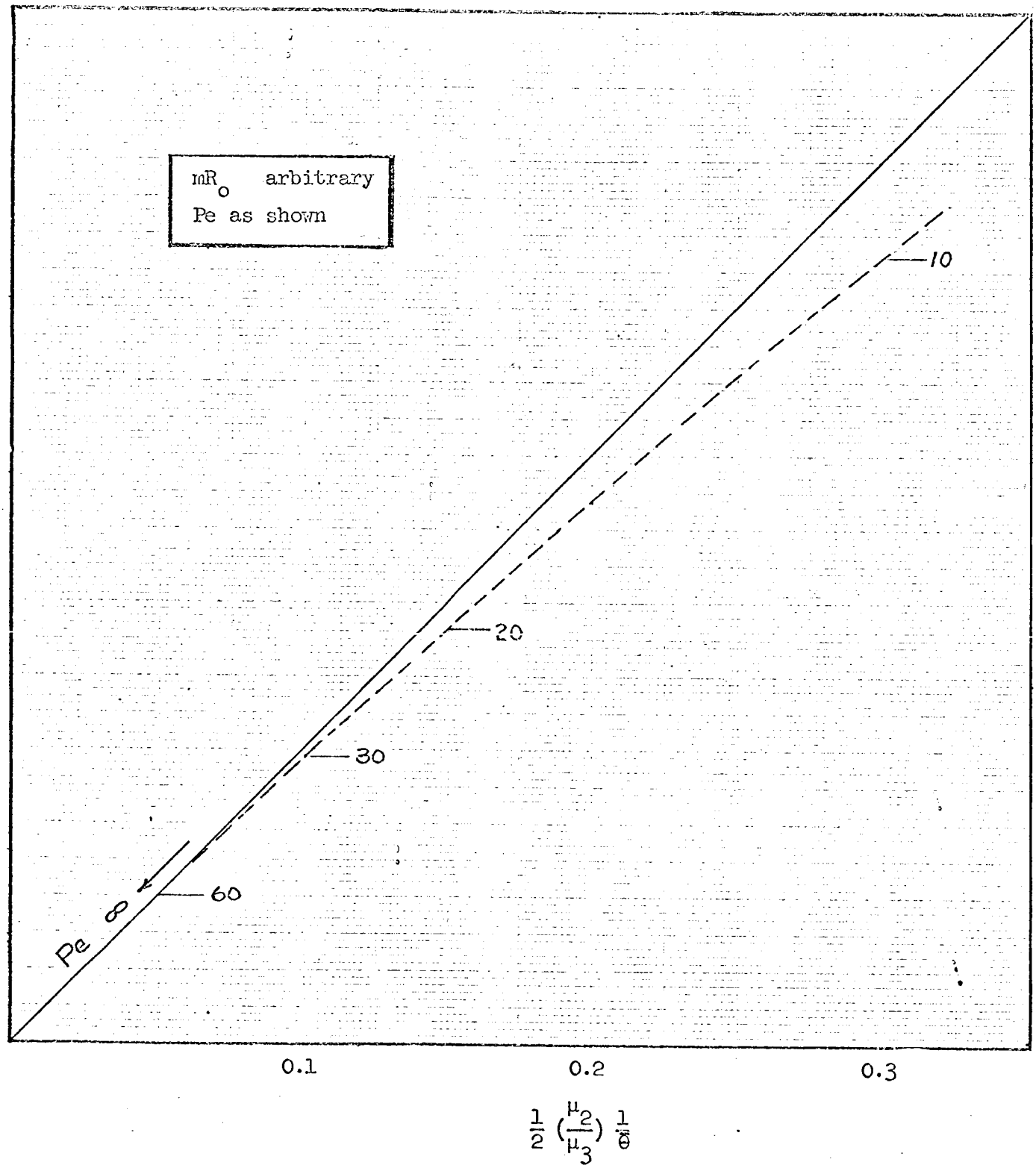

FIGURE 17. Correlation of Chromatogram Peak

$(0.02 \leq m\ R_o \leq 4.0)$, which are reasonable limits for practical chromatographic columns, at least 94% of the area of the chromatogram was encompassed in the time interval $(\theta_{max} \pm 2\sigma_{max})$. Fig. 18 shows results for two values of the diffusional parameter Pe.

In summary, it appears possible to estimate the basic characteristics of the chromatogram, knowing only the moments which can be computed from the column parameters. Activities remaining in this task include the numerical evaluation of the more complete model derived from the Lapidus-Amundson work and the application of the moment concept to it. Computational procedures for the model which contains integrals of modified Bessel functions and complicated exponentials are now underway.

Task E.2. Transport Parameter Estimation - D.A. Reichman
Faculty Advisor: Prof. P.K. Lashmet

When the development of the second order model of the chromatograph discussed above has been completed, the usefulness of the final equation will depend upon the availability of methods for estimating the model parameters, N_{tOG} and Pe. Methods for estimating N_{tOG} have been discussed earlier, Ref. 18, so this task has as its objective the development of a suitably accurate method for the estimation of the Peclet number Pe.

The Peclet number, which is a dimensionless measure of diffusion or dispersion in the directions of carrier gas flow, is defined as

$$Pe = \frac{vL}{D}$$

in which

v = velocity of the carrier gas
L = column length
D = diffusion constant

The diffusion constant D has, in general, both turbulent and molecular components. However, as the carrier gas velocity approaches zero, the diffusivity approaches the molecular diffusivity. Note that with no diffusion or dispersion, Pe becomes infinite, and the second order model reduces to the first order model investigated earlier, Ref. 18.

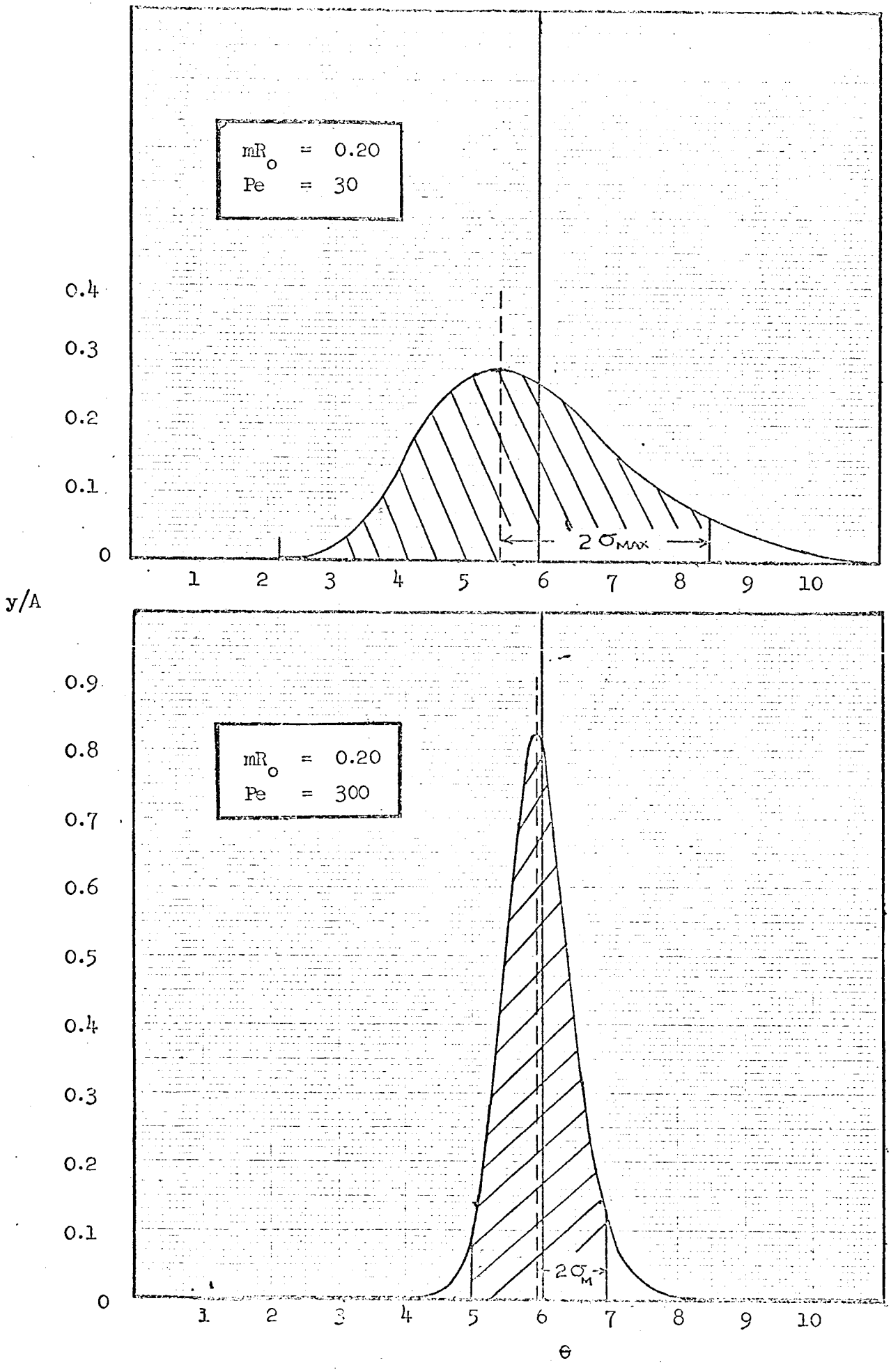

FIGURE 18. Typical Spread of a Chromatogram About the Mode

Initially, efforts were concentrated in two areas. First, a literature search was conducted to uncover existing correlations which could be applied to the envisioned chromatographic systems. Although many correlations were found, they were of limited use. The lowest Reynolds numbers

$$Re = \frac{d\ v\ \rho}{\mu}$$

in which

d = particle diameter
v = carrier gas velocity
ρ = carrier gas density
μ = carrier gas viscosity

were about 0.05 with most of the data for Reynolds numbers greater than 10. The Reynolds number (which is indicative of the fluid mechanics of the system) should be in the range ($0.01 \leq Re \leq 0.10$) for this project. Extrapolation of these curves to lower Reynolds numbers was not considered advisable because, at the low flow rates, molecular diffusion contributes significantly to the dispersion process, and the correlation curves should change radically.

In the second area of investigation, an attempt was to use simple geometric models of the column to predict dispersion by a statistical means. These models, Ref. 24, included a random walk model and rest phase/motion phase model. It was determined that these models could produce only order-of-magnitude solutions so the approach was abandoned.

The final choice of an estimation technique was based on the work of Johnson, Ref. 25, and Rhodes, Ref. 26. Basically the method compares two dispersion models through their statistical moments to arrive at an estimate of the Peclet number. The first model is the dispersed plug flow model of Aris, Ref. 27. This model allows observed behavior to be related to the dispersion number. The second model is the developed flow, continuum model of Bischoff, (Ref. 28) which allows the dispersion number to be related to the velocity profile in the bed. The velocity profile is estimated by the Rhodes technique, Ref. 26.

A computer subroutine has been written which computes the Peclet number based on the above techniques using as input data, the physical and chemical

properties of the system. These properties include mean particle diameter, particle size range, column diameter and length, carrier gas velocity and the physical properties of the carrier gas like density. The program results will be checked with some of the original dispersion data and some recently reported data at low Reynolds numbers, Ref. 29.

This subroutine is to be considered as a "transport parameter" program, so it will include N_{tOG} estimating methods discussed earlier, Ref. 18. This parameter is also a function of many of the physical parameters noted above.

In addition to the preparation of the computational methods, the task will present design curves, for rapid estimation of Pe and N_{tOG}. These will be useful in preliminary system analysis such as those being developed by the moment analysis techniques.

Task E.3. Sample Injection Problem - R.C. Krum
Faculty Advisor: Prof. P.K. Lashmet

It was the objective of this task to investigate the effect of finite injection time of the sample upon the chromatogram. Initial studies on the first-order model with an impulse injection, Ref. 18, showed that the model represented an actual chromatogram quite poorly. Since an impulse injection is mechanically impossible, the task was concerned with evaluating the effects of finite injection time which could account for some of the discrepancy, Ref. 30.

To obtain an estimate of the effect of finite injection time upon column performance, a rectangular pulse was mathematically convoluted with the impulse solution to the system equations. Although some work was done with the first order model, the second order equilibrium adsorption model was selected for the major studies as it was more representative of system performance, Fig. 16. Fig. 19 shows the effect of two different pulses upon the chromatogram. The variables studied included injection time, the Peclet number Pe, and the thermodynamic function m R_o. Typical results are shown in Fig. 20. The abscissa represents the ratio of the injection time θ_τ to the time the theoretical peak emerges from the column θ_m. The ordinate is the ratio of the peak height for the pulse injection to the peak height for the impulse forcing function. Since the areas under these chromatograms must be

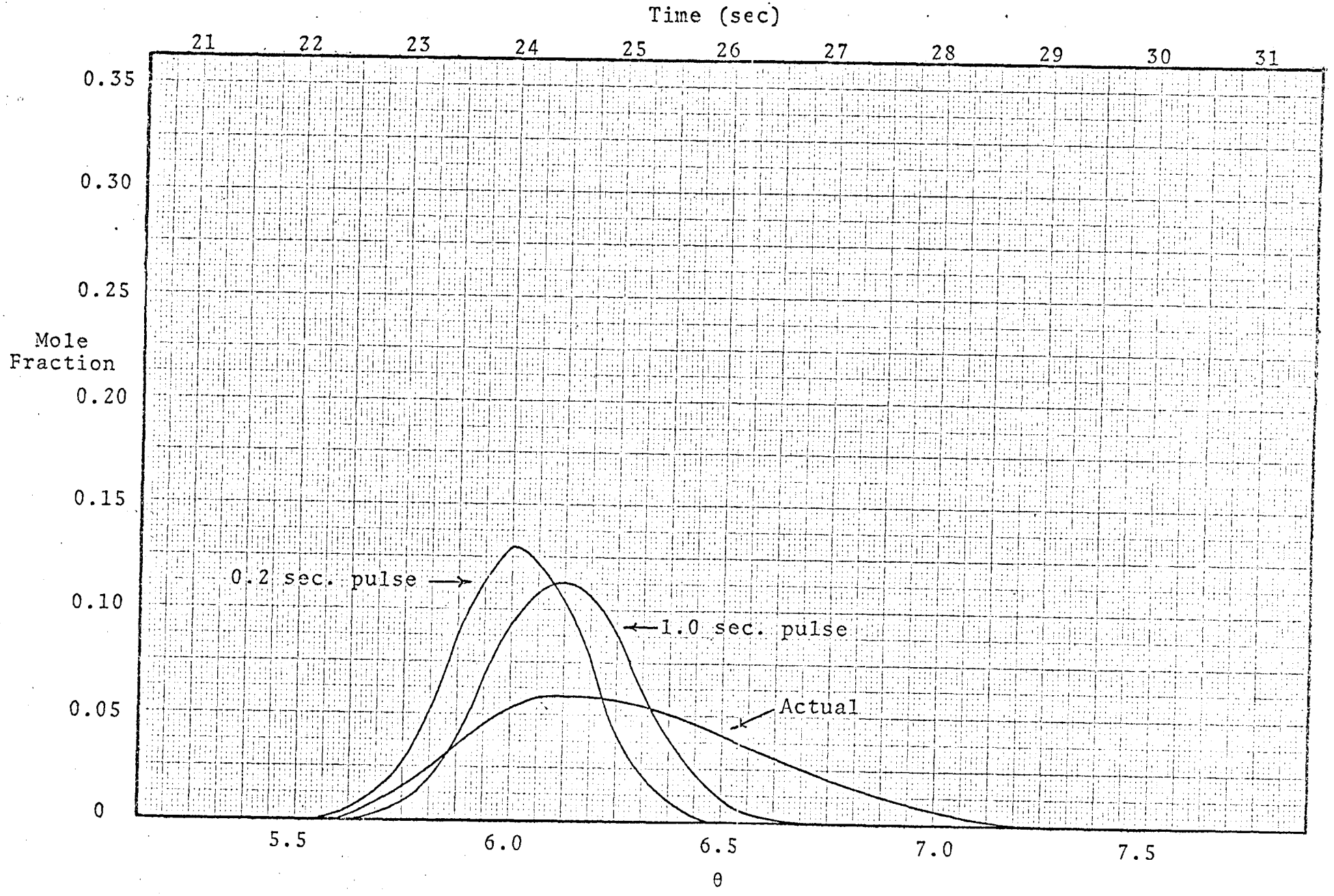

Figure 19. Comparison of the equilibrium adsorption model and pentane chromatogram.
mR_o = 0.2, Pe = 3000, A(t) = 0.05

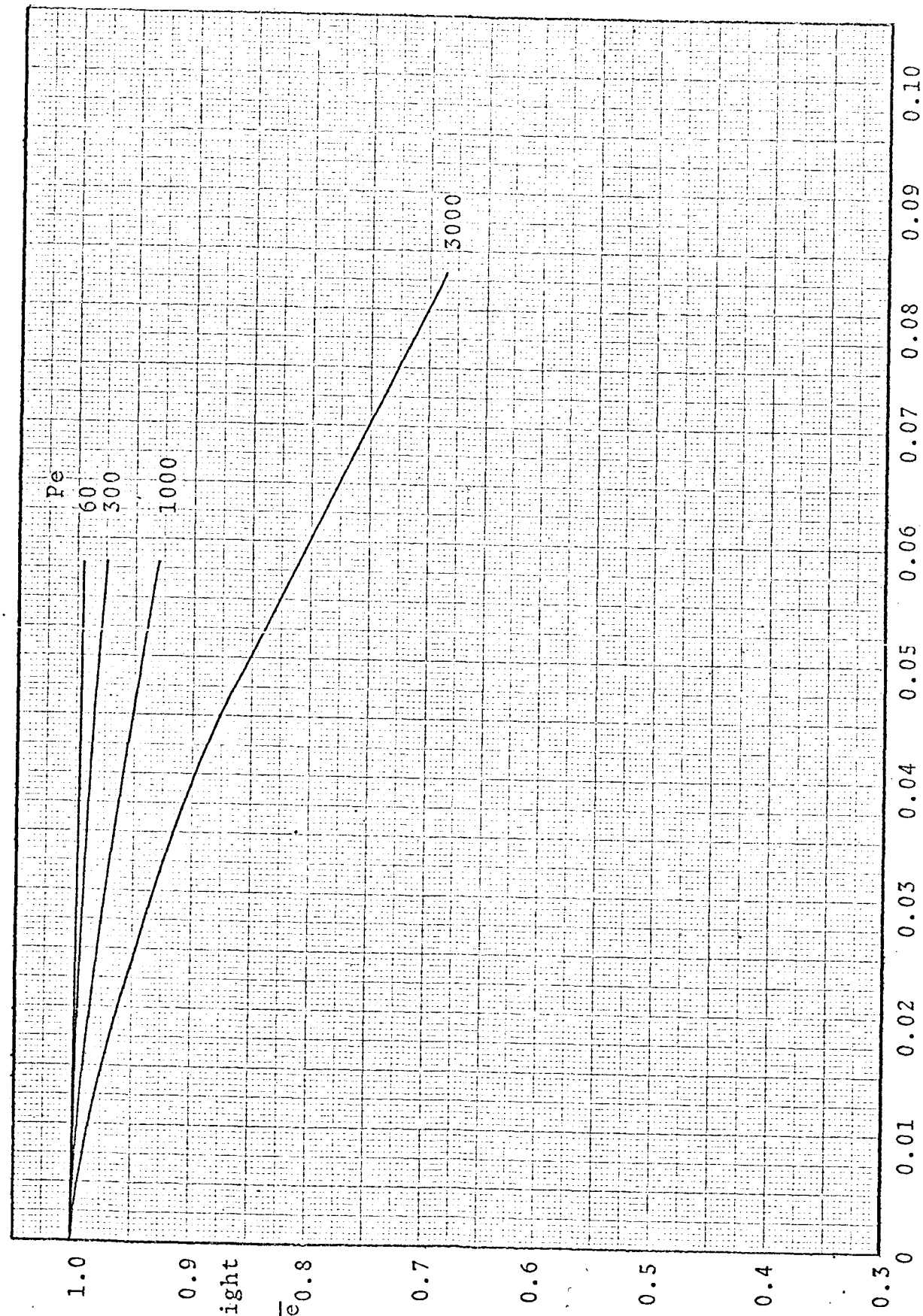

Figure 20. Effect of Pe on resolution - equilibrium adsorption model.

$mR_o = 0.2$

equal (the area is proportional to the amount of sample injected), the ordinate is also related to the peak spreading.

In general, it was concluded that increasing the injection time had two effects upon the chromatogram. First, because the injection function was more diffuse than the impulse, the output or chromatogram was broader and shorter. More broadening occurred as Pe and mR_o increased. In general, the sharper the theoretical impulse peak, the quicker the injection time caused a loss in resolution. The second noticeable effect of injection time was the delay in the appearance of the peak. This was caused by the finite amount of time required to complete the total injection of the sample. Since the total sample was not inside the column until a time Θ_τ after injection began, the maximum point of the output was delayed from the impulse peak time by about Θ_τ.

A final correlation of these effects is useful for design purposes is given in Fig. 21. These curves show the maximum injection time allowable for a 10% reduction in peak height for various values of Pe and mR_o. It should be noted that these curves are for the second-order, equilibrium adsorption model (N_{tOG} being infinite). For finite values of N_{tOG}, the curves are expected to move toward the right. In other words, the allowable injection times are conservative.

The tasks thus far have developed methods for approximating the chromatogram characteristics through moment analysis and have shown limitations imposed by finite sample injection time. The transport parameter computations should be completed in early in the next period. Tasks to be pursued in the next period include the following:

1. Evaluation of the more complete second order model via computational means and comparison with data.

2. Extension of the concepts to samples containing several chemical species.

3. Evaluation of the effect of large amounts of solvent upon detection of minute quantities of materials.

In addition to these studies, a chromatographic test system is being constructed by renovating a Perkin-Elmer,

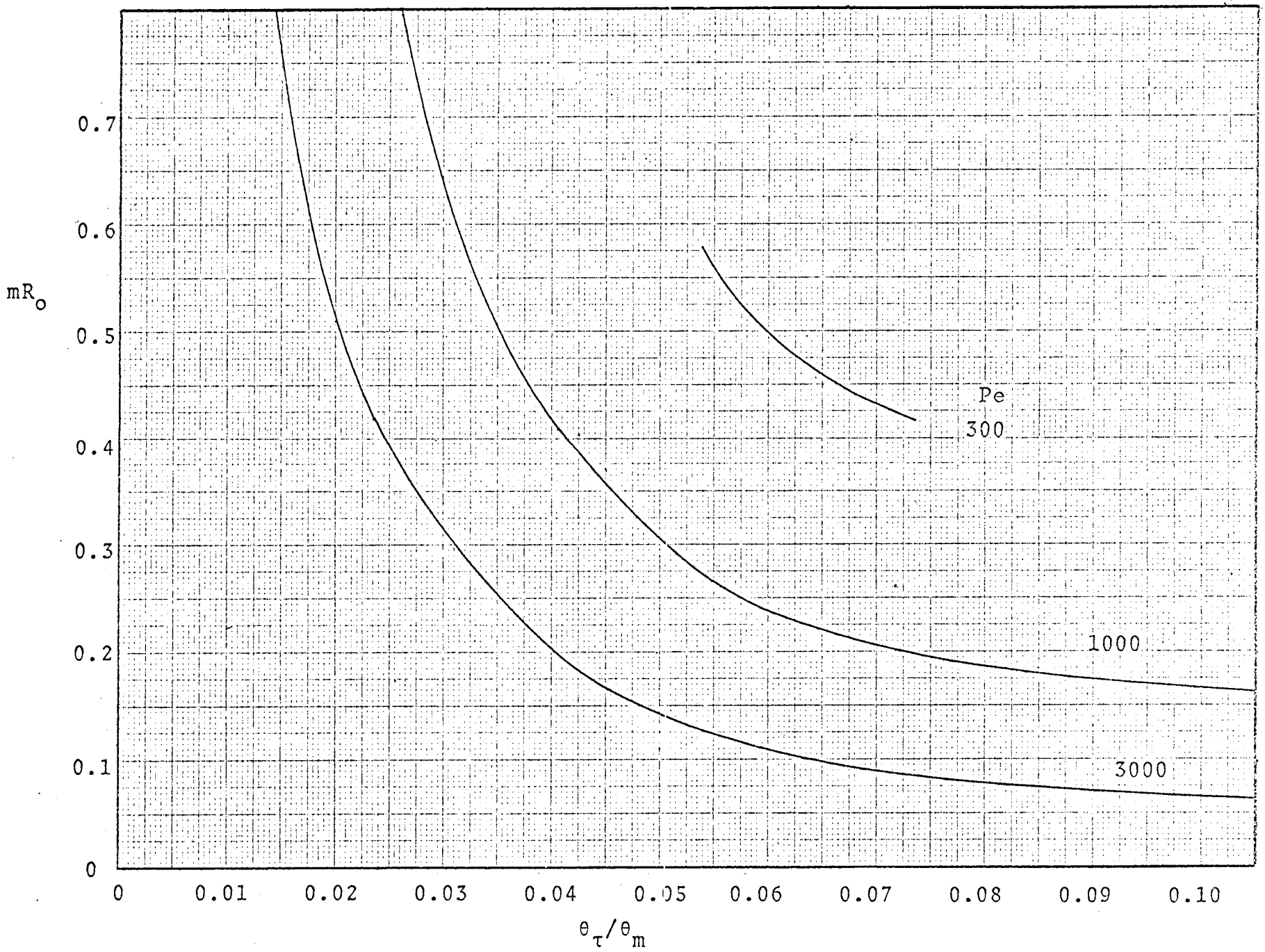

Figure 21. Effect of mR_o on θ_τ - equilibrium adsorption model. Peak Height $\frac{\text{Pulse}}{\text{Impulse}}$ = .9

Model 154-C chromatograph. New detectors having 0.04 second time constants and other equipment have been obtained and are being installed. The equipment should be operational by early fall, 1969.

IV. Projections of Activity for the Period July 1, 1969 to June 30, 1970

The following activities are projected for the coming period:

1. The atmospheric parameter updating and adaptive trajectory control tasks will be phased out by September 1969 and a summary report bringing the several studies undertaken in the past in this area into a proper perspective will be prepared.

2. The feasibility of the use of the rotary wing (autogyro) concept for an unpowered landing on Mars will be determined. The decisions as to further work along these lines will depend not only on the outcome of this study, which is expected to be completed by October 1969, but also on the question of allocation of resources between this task and other pressing problems related to the landed mobile vehicle, (see item 6 below).

3. Emphasis will continue to be directed to problems related to terrain modeling for purposes of defining terrain sensor requirements and developing and evaluating path selection algorithms.

4. With the development of unambiguous relationships between measurable detector deflections and the Euler angles without the limitation of small angles as reported herein, effort will be directed to the analysis of the dynamics of attitude sensors and to the design of an attitude control and/or navigation system.

5. The use of Mars orbiters for navigation of the mobile vehicle will be investigated. The initial effort which will be concentrated on problems related to the location of the orbiters will be followed by studies concerned with the vehicle, the target destination and obstacles.

6. A major effort relating to the design of a mobile vehicle will be initiated. Problems related to vehicle configuration, propulsion, power sources, suspension system, vehicle stability, control and guidance will be considered.

7. The chromatographic system studies will be extended to include: evaluation of theoretical models including experimental studies, multicomponent separations problems, and the effect of large amounts of solvent upon the detection of minute quantities of materials.

V. Educational Considerations

In addition to the technical goals outlined earlier, this project has the objective of promoting the education of engineering students in directions and dimensions not normally encountered in formal programs of study. In brief, the project activity provides real problems of substance whose solution is obtained not by the application of expedient simplifications to make them manageable but rather according to the technical needs that realistically apply to the situation. Accordingly, the students learn to accommodate to trade-offs between competing values and to work with boundary conditions and constraints originating with the factual situation and which may be compounded by the interfacing of tasks. In this type of environment, the student perceives that his role in professional practice will normally involve a significant amount of interaction with other individuals and that his work cannot proceed independently and without consideration of and impingement by the work of others. Furthermore, he is forced to obtain, understand and utilize knowledge which is on occasion far removed from his own speciality field and to undertake research when necessary to obtain the required information. Although the very nature of the problems and the faculty perspective emphasize the relevance and importance of the technical goals, the periodic visits of Mr. Eric Suggs of Jet Propulsion, and on occasion of other NASA representatives, to review progress reinforce these concepts dramatically.

From an educational point of view, the project has proven to be an unqualified success. Large numbers of students (approximately 40 in two years) have had the unique experiences of real-life involvement in engineering problems within the context of their formal education.

Pertinent information regarding the participating students, their degree goals or achievements, the period of participation and their support relationship to the project is summarized below. While this information may be of general interest, its primary value insofar as this progress report is concerned is that it provides a basis for evaluation of the progress made in individual task areas. It should be noted that all students are meeting an academic requirement by this activity.

The following students met their degree objectives since July 1, 1968:

			Method of Support
R. Carron	M. Eng.	(Mech.Eng.)	Cluett-Peabody Fellowship
P. Cefola	Ph.D. Eng.	(Mech.Eng.)	Project Support(1)
A. Himmel	M. Eng.	(Elec.Eng.)	NSF Fellowship
R. Janosko	M. Eng.	(Mech.Eng.)	Project Support(1)
J. Jendro	M. Eng.	(Mech.Eng.)	NSF Fellowship
R. Krum	M. Eng.	(Chem.Eng.)	DuPont Traineeship
J. Lazzara	M. Eng.	(Mech.Eng.)	Teaching Assistant
J. Mleziva	M. Eng.	(Elec.Eng.)	Teaching Assistant
J. Morgan	B.S.	(Mech.Eng.)	Partial Project Support(2)
N. Pinchuk	M. Eng.	(Elec.Eng.)	Teaching Assistant
J. Sadler	M. Eng.	(Mech.Eng.)	Teaching Assistant
T. Sliva	M. Eng.	(Chem.Eng.)	Self-supported
W. Voytus	M. Eng.	(Chem.Eng.)	NSF Fellowship
R. Wepner	M. Eng.	(Mech.Eng.)	NASA Fellowship

The following students will continue on the project for varying periods of time to achieve the indicated degree objectives:

L. Hedge	M. Eng.	(Mech.Eng.)	Project Support(1)
J. Hudock	M. Eng.	(Elec.Eng.)	Partial Project Support(3)
R. Janosko	Ph.D. Eng.	(Mech.Eng.)	Project Support(1)
T. Kershaw	Ph.D. Eng.	(Mech.Eng.)	Partial Project Support(4)
J. LaBarbara	M. Eng.	(Elec.Eng.)	Project Support(1)
J. Lazzara	Ph.D. Eng.	(Mech.Eng.)	Teaching Assistant
R. Mancini	M. Eng.	(Elec.Eng.)	Project Support(1)
D. Reichman	M. Eng.	(Chem.Eng.)	Project Support(1)
P. Rayfield	Ph.D. Eng.	(Mech.Eng.)	Partial Project Support(5)

(1) Stipend plus tuition support.
(2) Ten hours per week support for one term.
(3) Stipend plus tuition for one term.
(4) Summer support only.
(5) Summer support plus stipend and tuition for one term.

REFERENCES

1. Janosko, R.E., "On-Line Parameter Updating of the Martian Atmosphere with Minimum Storage", R.P.I. Technical Report MP-2, Rensselaer Polytechnic Institute, Troy, New York, January 1969.

2. Cefola, P.J., "Sensitivity Guidance for Entry into an Uncertain Martian Atmosphere", Ph.D. Thesis, Rensselaer Polytechnic Institute, Troy, New York, November 1968.

3. Hedge, L.F., "Trajectory Control for Mars Entry by Discrete Changes of Drag Surface and Flight Path", R.P.I. Technical Report MP-5, Rensselaer Polytechnic Institute, Troy, New York, August 1969.

4. Shen, C.N. and P.J. Cefola, "Adaptive Trajectory Control for Mars Entry Based on Sensitivity Analysis", AIAA 68-835, AIAA Guidance, Control and Flight Dynamics Conference, Pasadena, Calif., August 1968. (Accepted for publication in the AIAA Journal).

5. Cefola, P.J. and C.N. Shen, "Vector-Matrix Second Order Sensitivity Equations with Applications to Mars Entry", Presented at the Second Hawaii International Conference on Systems Sciences, January 1969. (Accepted for publication in the AIAA Journal).

6. Carron, R.J., "Extension of Parameter Updating System for Atmospheric Density Determination to the Regions above the Tropopause", M. Eng. Project Report, Rensselaer Polytechnic Institute, Troy, New York, June 1969.

7. Rayfield, W.P., "Autogyro Rotor-Hub Assembly Design," R.P.I. Technical Report MP-7, Rensselaer Polytechnic Institute, Troy, New York. (To be issued October 1969).

8. Wepner, R., "Blade Support and Pitch Control for the Unpowered Landing of the NASA Mars Voyager Vehicle", M. Eng. Project Report, Rensselaer Polytechnic Institute, Troy, New York.

9. Saddler, J.P., "The Study of an Inflatable Rotor Blade for Use in a Mars Landing by Autogyro", M. Eng. Project Report, Rensselaer Polytechnic Institute, Troy, New York, June 1969.

10. Frederick, D.K., Lashmet, P.K., Sandor, G.N., Shen, C.N., Smith, E.J., and Yerazunis, S.W., Progress Report

July 1, 1969 to Dec. 31, 1969, "Analysis and Design of a Capsule Landing System and Surface Vehicle Control System for Mars Exploration", Technical Report MP-3, Rensselaer Polytechnic Institute, Troy, New York, February 1969.

11. Lashmet, P.K., Lee, I., Sandor, G.N., Shen, C.N., Smith, E.J. and Yerazunis, S., Progress Report Jan.1, 1968 to June 30, 1968, "Analysis and Design of a Capsule Landing System and Surface Vehicle Control System for Mars Exploration", Rensselaer Polytechnic Institute, Troy, New York, June 1969.

12. LaBarbara, J., "Short Range Obstacle Detection System", R.P.I. Technical Report MP-6, Rensselaer Polytechnic Institute, Troy, N.Y. (To be issued September 1969).

13. Hudock, J., "Transient Analysis of Vehicle Suspension System", R.P.I. Technical Report MP-8, Rensselaer Polytechnic Institute, Troy, New York (To be issued September 1969).

14. Himmel, A., "Large Angle Gyro Sensing System", M. Eng. Project Report, Rensselaer Polytechnic Institute, Troy, New York, June 1969.

15. Jendro, J., "Attitude Sensing Utilizing a Pendulous System", M. Eng. Project Report, Rensselaer Polytechnic Institute, Troy, New York, June 1969.

16. Mleziva, J., "Pendulous Attitude Sensing System", M. Eng. Project Report, Rensselaer Polytechnic Institute, Troy, New York, June 1969.

17. Pinchuck, N., "Design of Large Angle Attitude Sensor for Mars Rover", M. Eng. Project Report, Rensselaer Polytechnic Institute, Troy, New York, June 1969.

18. Sliva, T.F., "Chromatographic Systems Analysis: First-Order Model Evaluation", M. Eng. Project Report, Rensselaer Polytechnic Institute, Troy, New York (1968).

19. Lapidus, L., and Amundson, N.R., "Effect of Longitudinal Diffusion in Ion Exchange and Chromatographic Columns", J. Phys. Chem., 56, 984 (1952).

20. Grubner, O., Zekanova, A., and Rolek, M., "Statistical Moments Theory of Gas-Solid Chromatography, Diffusion Controlled Kinetics", J. Chromatography, 28, 209 (1967).

21. Kucera, E., "Linear Non-Equilibrium Chromatography", J. Chromatography, 19, 237 (1965).

22. Yamazaki, H., "A Mathematical Treatment of Non-Equilibrium Chromatography", J. Chromatography, 27, 14 (1967).

23. Voytus, W.A., "Chromatographic Systems Analysis: Moment Analysis of the Equilibrium Adsorption Model", M. Eng. Project Report, Rensselaer Polytechnic Institute, Troy, New York (1969).

24. Taylor, G.I., "Dispersion of Soluble Matter in a Solvent Flowing Slowly Through a Tube," Proc. Royal Soc. (London), A219, 186 (1953).

25. Johnson, G., "Axial Dispersion from Flow Non-Uniformities in Packed Beds", Ph.D. Dissertation, Rensselaer Polytechnic Institute, Troy, New York (1967).

26. Rhodes, R., "Flow of Air in Beds of Spheres, a Statistical and Theoretical Approach", Ph.D. Dissertation, Rensselaer Polytechnic Institute, Troy, New York (1963).

27. Aris, R., "On the Dispersion of a Solute in a Fluid Flowing through a Tube", Proc. Royal Soc. (London), A235, 67 (1956).

28. Bischoff, K.B., and Levenspiel, O., "Fluid Dispersion: Generalization and Comparison of Mathematical Models", Chem. Eng. Sci., 17, 245, 257 (1962).

29. Balla, L.Z., and Weber, T.W., "Axial Dispersion of Gases in Packed Beds", A.I. Ch.E. J., 15, 146 (1969).

30. Krum, R.C., "Chromatographic Systems Analysis: Sample Injection Problem", M. Eng. Project Report, Rensselaer Polytechnic Institute, Troy, New York (1969).